Impact of Z' and UED parameters on different asymmetries in $B_s \rightarrow \phi \ell^+ \ell^-$ decays

Ishtiaq Ahmed^{1,2}, * M. Jamil Aslam^{1,2}, † and M. Ali Paracha^{3,4‡}

¹National Centre for Physics,

Quaid-i-Azam University Campus,

Islamabad 45320, Pakistan

 $^{2}Department$ of Physics,

Quaid-i-Azam University, Islamabad 45320, Pakistan

³Centre for Advanced Mathematics and Physics, National University of Science and Technology.

Islamabad, Pakistan and

⁴Laboratòrio de Fsica Teòrica e Computacional, Universidade Cruzeiro do Sul, 01506-000 São Paulo, Brazil

(Dated: February 25, 2022)

A comprehensive study of the impact of new-physics on different observables for $B_s \to \phi \ell^+ \ell^-$ has been done. We examine the new physics models such as Z' and UED models, where the effects of new physics coming through the modification of Wilson coefficients. We have analyzed these effects through the theoretical prediction of the branching ratio, the forward-backward asymmetry, lepton polarization asymmetries and the helicity fractions of the final state meson. These all observables will definitely be measured in present and future colliders with great precision. We also pointed out that hadronic uncertainties in various physical observables are small which make them an ideal probe to establish new physics. Therefore, the measurements of these observables for the same decay would permit the detection of physics beyond the Standard Model and will also help us to distinguish between different new physics scenarios.

I. INTRODUCTION

Studies of flavor-changing neutral current (FCNC) decays have played a pivotal role in formulating the theoretical description of particle physics known as the Standard Model (SM). In the SM, at tree level, all the neutral currents conserve flavor so that FCNC decays do not occur at lowest order and are induced by the Glahsow-Iliopoulos-Maiani (GIM) amplitude [1] at the loop level, which make their effective strength small. In addition to this loop suppression these are also suppressed in the SM due to their dependence on the weak mixing angles of the Cabbibo-Kobayashi-Maskawa (CKM) matrix V_{CKM} [2, 3]. Therefore, these two circumstances make the FCNC decays relatively rare and hence important to provide stringent tests of SM in the flavor sector.

Although many measurements of observables in the B meson systems agree with the SM. However, there are several observables whose measured values differ from the predictions of the SM such as (i) the values of $B_d^0 - \bar{B}_d^0$ mixing phase sin (2β) obtained from different penguin dominated $b \to s$ channels tend to be systematically smaller than that obtained from $B_d^0 \to J/\psi K_s$ [4–6], (ii) the $B_s^0 - \bar{B}_s^0$ mixing phase by the CDF and D0 collaboration deviates from the SM prediction [7, 8], (iii) in $B \to K\pi$ decays, it is difficult to account for all the experimental measurements within the SM [9], (iv) the isospin asymmetry between neutral and the charged decay modes of the $\bar{B} \to \bar{K^*}\ell^+\ell^-$ decay also deviate from the SM [10]. These disagreements are typically at the level 2σ which are not statistically significant, but still these are fertile ground to test SM and check the NP, as they appear in the $b \to s$ transitions. In this context there have been numerous papers examining the possible new physics (NP) FCNC scenarios through the various $b \to s$ processes [11].

On the experimental side, the Large Hadron Collider (LHC) is already up and running where CMS, ATLAS and LHCb have started taking data while the Belle II is on its way. We are already witnessing that SM is still standing tall at least in the data taken till to date and the recent discovery of Higgs like boson in the mass range of 126GeV has left enough air to breath for the SM. It is therefore an ideal time to test the predictions of SM and try to identify the nature of physics that is beyond it.

Moreover, in the SM the zero crossing of the leptons forward-backward asymmetry $(A_{FB}(q^2))$ in $B \to K^* l^+ l^$ is at a well determined position which is free from the hadronic uncertainties at the leading order (LO) in strong coupling α_s [12–14]. On the other hand the LHCb has announced the results of A_{FB} , the fraction of longitudinal

^{*}Electronic address: ishtiaq@ncp.edu.pk

 $^{^{\}dagger}\mbox{Electronic}$ address: jamil@phys.qau.edu.pk

[‡]Electronic address: ali@ncp.edu.pk

2

polarization F_L and the differential branching ratio dB/dq^2 , as a function of the dimuon invariant mass for the decay $\bar{B} \to \bar{K}^* \mu^+ \mu^-$ using 0.37fb⁻¹ of data taken in the year 2011 [15]. These results of $A_{FB}(\bar{B} \to \bar{K}^* \mu^+ \mu^-)$ are close to the SM predictions with slight error bars, thus they have overwritten the earlier measurements by Babar and Belle which measure this asymmetry with opposite sign with better statistics [15–18]. The collaboration plans to continue to the study of the channel $\bar{B} \to \bar{K}^* \mu^+ \mu^-$ in finer detail, with more angular variables, and expected to achieve high sensitivity to any small deviation from the SM [15].

In order to incorporate the experimental predictions of different physical observables in $\bar{B} \to \bar{K}^* \mu^+ \mu^-$ this decay has been studied in SM and in number of different NP scenarios [19, 20, 22–40] where NP effects display themselves through modification in the Wilson coefficients as well as through the new operators. Beside these models the general analysis of $\bar{B} \to \bar{K}^* \mu^+ \mu^-$ decay has also been performed which allow us to include all possible NP operators such as vector-axial vector (VA), scalar-pseudoscalar (SP) and tensor-axial tensor (TE) [41].

Apart from the ordinary B meson decays an interesting avenue for the NP is opened by the B_s meson decays, where $B_s^0 - \bar{B}_s^0$ mixing is the exciting feature, which in the SM, is originated from the box topologies and hence is strongly suppressed. In the presence of NP, new particles could give rise to additional box topologies or even these decays can occurs at the tree level. In this regard, the key channel to address this possibility is the $B_s^0 \to J/\Psi\phi$ where the pertinent feature is that its final state contains two vector mesons and thereby require the time dependent angular analysis of the $J/\Psi \to \mu^+\mu^-$ and $\phi \to K^+K^-$ decay products [42]. In addition, over the last couple of years, measurements of CP violating asymmetries in "tagged" analysis (distinguishing between initially present B_s^0 or \bar{B}_s^0 mesons) of the $B_s^0 \to J/\Psi\phi$ channel at the Tevatron indicate possible NP effects in $B_s^0 - \bar{B}_s^0$ mixing [43–45]. These results are complemented by the measurement of the anomalous like-sign dimuon charge asymmetry at D0, which was found to differ by 3.9σ from the SM prediction [46]. However, in the last summer the LHCb collaboration has also reported, the results that disfavor large NP effects [47]. Therefore, the more data is needed to clarify the potential and status of NP.

Following the same footprints, the exclusive $B_s \to \phi \ell^+ \ell^-$ become also attractive since at quark level these decays are also induced by $b \to s \ell^+ \ell^-$, and could be measured at the running Tevatron, LHC and future super-B factories. Recently, the CDF collaboration had observed $B_s \to \phi \mu^+ \mu^-$ with the branching ratio [41]

$$Br(B_s \to \phi \mu^+ \mu^-) = [1.44 \pm 0.33(\text{stat.}) \pm 0.46(\text{syst.})] \times 10^{-6}.$$
 (1)

On theoretical side this exclusive process is well studied in the literature [48–52] with varying degrees of theoretical rigor and emphasis. In order to study different physical observables such as, dilepton invariant mass spectrum, the forward-backward asymmetry, helicity fractions of final state meson and different lepton polarization asymmetries, the crucial ingredients are the form factors which needed to be calculated using a non-perturbative QCD methods and therefore form the bulk of theoretical uncertainties. Form factors parameterizing $B_s \rightarrow \phi \mu^+ \mu^-$ have already been calculated in different models, such as light cone sum rules (LCSRs) [53–55], perturbative QCD approach [56], relativistic constituent quark model [57], constituent quark model [58] and light front quark model [59]. Among them, the LCSRs deal with form factors at small momentum region and is complementary to the lattice QCD approach and consistent with perturbative QCD as well as heavy quark limit, therefore, we will adopt the form factors calculated by this approach in our forthcoming analysis of $B_s \rightarrow \phi \ell^+ \ell^-$ decays in the SM and two different NP models, namely, Z' and Universal Extra Dimension (UED). The form factors calculated from LCSRs are restricted to the low q^2 region, where at the high q^2 region, ongoing efforts aim at the first unquenched prediction from lattice [60].

It is well known that the NP play its role in the rare B meson decays in two different ways, one is through the modification in the Wilson coefficients corresponding to the SM operators and the other is due to the appearance of new operators in the effective Hamiltonian, which are absent in the SM. The UED and Z' models' belong to the category, commonly known as Minimal Flavor Violating models, which do not change the operator basis of the SM and hence their contribution is absorbed in the Wilson coefficients. In the present study, we perform the analysis of branching ratio, the forward-backward asymmetry (A_{FB}) , the helicity fraction of final state ϕ meson $(f_{L,T})$, the lepton polarization asymmetries (both single and double) in the $B_s \to \phi \ell^+ \ell^-$ decay in aforementioned NP scenarios.

The outline of the paper is as follows: In Sec. 2 we briefly discuss the different NP scenarios and introduce the effective Hamiltonian formalism for semileptonic rare B_s decays. Section 3 contains the definitions and parameterizations of $B_s \rightarrow \phi$ matrix elements and summarizes the form factor calculated in LCSRs. In Sec. 4, we display the mathematical expressions for the branching ratio, the forward-backward asymmetry, the helicity fractions of ϕ meson and the different lepton polarization asymmetries. Sec. 5 contains our numerical results for the above mentioned physical observables both in the SM and in different NP scenarios where we show the influence of the NP parameters on the various asymmetries outlined above. A brief summary and some concluding remarks are also given at the end of this section.

II. THEORETICAL FRAMEWORK

To calculate the decay amplitude of $B_s \to \phi \ell^+ \ell^-$ decays requires some theoretical steps. Among them the most important and relevant are:

- the separation of short distance effects (encoded in Wilson coefficients) from the long-distance QCD effects (encoded in the matrix elements) in the effective Hamiltonian;
- the calculation of matrix elements of local quark bilinear operators of the type $\langle \phi | J | B_s \rangle$ in terms of form factors.

As the effective Hamiltonian will be changed in different models therefore at first step we will describe the effective Hamiltonian in the aforementioned models and the discussion about the form factors will be postponed to next section.

A. Standard Model (SM)

At quark level the decay $B_s \to \phi \ell^+ \ell^-$ is governed by the transition $b \to s \ell^+ \ell^-$ for which the effective Hamiltonian can be written as

$$H_{eff} = -\frac{4G_F}{\sqrt{2}} V_{tb}^* V_{ts} \sum_{i=1}^{10} C_i(\mu) O_i(\mu), \qquad (2)$$

where $O_i(\mu)$ (i = 1, ..., 6) are the four-quark operators, i = 7, 8 are dipole operators and i = 9, 10 are the semileptonic operators. The $C_i(\mu)$ are the corresponding Wilson coefficients at the energy scale μ . The terms that corresponds to the running of *u*-quark in the loop, i.e. $V_{ub}^* V_{us}$ can be safely ignored because $\frac{V_{ub}^* V_{us}}{V_{tb}^* V_{ts}} \prec 2 \times 10^{-2}$. The operators responsible for $B_s \rightarrow \phi \ell^+ \ell^-$ are O_7 , O_9 and O_{10} and their form is given by

$$O_{7} = \frac{e^{2}}{16\pi^{2}} m_{b} \left(\bar{s}\sigma_{\mu\nu} P_{R} b \right) F^{\mu\nu},$$

$$O_{9} = \frac{e^{2}}{16\pi^{2}} (\bar{s}\gamma_{\mu} P_{L} b) (\bar{l}\gamma^{\mu} l),$$

$$O_{10} = \frac{e^{2}}{16\pi^{2}} (\bar{s}\gamma_{\mu} P_{L} b) (\bar{l}\gamma^{\mu}\gamma_{5} l),$$
(3)

with $P_{L,R} = (1 \pm \gamma_5)/2$. The Wilson coefficients C_i can be calculated perturbatively and the explicit expressions of these in the SM at next-to-leading order (NLO) and at next-to-next leading logarithm (NNLL) are given in [61–76]. Since the Z -boson is absent in the effective theory, therefore the operator O_{10} can not be induced by the insertion of four-quark operators. Hence, the Wilson coefficient C_{10} does not renormalize under QCD corrections and so it is independent on the energy scale.

The Wilson coefficient $C_9^{SM}(\mu)$ which is commonly written as $C_9^{eff}(\mu)$ corresponds to the semileptonic operator O_9 . It can be decomposed into three parts

$$C_9^{SM} = C_9^{eff}(\mu) = C_9(\mu) + Y_{SD}(z, s') + Y_{LD}(z, s'), \tag{4}$$

where the parameters z and s' are defined as $z = m_c/m_b$, $s' = q^2/m_b^2$. The short distance function $Y_{SD}(z, s')$ describes the perturbative part which include the indirect contributions from the matrix element of four-quark operators $\sum_{i=1}^{6} \langle l^+ l^- s | O_i | b \rangle$ and this lies sufficiently far away from the $c\bar{c}$ resonance regions. The manifest expressions for $Y_{SD}(z, s')$ can be written as [62, 63]

$$Y_{SD}(z,s') = h(z,s')(3C_1(\mu) + C_2(\mu) + 3C_3(\mu) + C_4(\mu) + 3C_5(\mu) + C_6(\mu)) -\frac{1}{2}h(1,s')(4C_3(\mu) + 4C_4(\mu) + 3C_5(\mu) + C_6(\mu)) -\frac{1}{2}h(0,s')(C_3(\mu) + 3C_4(\mu)) + \frac{2}{9}(3C_3(\mu) + C_4(\mu) + 3C_5(\mu) + C_6(\mu)),$$
(5)

with

$$h(z,s') = -\frac{8}{9}\ln z + \frac{8}{27} + \frac{4}{9}x - \frac{2}{9}(2+x)|1-x|^{1/2} \begin{cases} \ln\left|\frac{\sqrt{1-x}+1}{\sqrt{1-x}-1}\right| - i\pi & \text{for } x \equiv 4z^2/s' < 1\\ 2\arctan\frac{1}{\sqrt{x-1}} & \text{for } x \equiv 4z^2/s' > 1 \end{cases},$$

$$h(0,s') = \frac{8}{27} - \frac{8}{9}\ln\frac{m_b}{\mu} - \frac{4}{9}\ln s' + \frac{4}{9}i\pi . \tag{6}$$

The long-distance contributions $Y_{LD}(z, s')$ from four-quark operators near the $c\bar{c}$ resonance cannot be calculated from first principles of QCD and are usually parameterized in the form of a phenomenological Breit-Wigner formula making use of the vacuum saturation approximation and quark-hadron duality. In the present study we ignore this part because this lies far away from the region of interest.

The non-factorizable effects [77–79] from the charm loop can bring about further corrections to the radiative $b \to s\gamma$ transition, which can be absorbed into the effective Wilson coefficient C_7^{eff} . Specifically, the Wilson coefficient C_7^{eff} is given by

$$C_7^{SM} = C_7^{eff}(\mu) = C_7(\mu) + C_{b \to s\gamma}(\mu), \tag{7}$$

with

$$C_{b\to s\gamma}(\mu) = i\alpha_s \bigg[\frac{2}{9} \eta^{14/23} (G_1(x_t) - 0.1687) - 0.03C_2(\mu) \bigg],$$
(8)

$$G_1(x_t) = \frac{x_t(x_t^2 - 5x_t - 2)}{8(x_t - 1)^3} + \frac{3x_t^2 \ln^2 x_t}{4(x_t - 1)^4},$$
(9)

where $\eta = \alpha_s(m_W)/\alpha_s(\mu)$, $x_t = m_t^2/m_W^2$, $C_{b\to s\gamma}$ is the absorptive part for the $b \to sc\bar{c} \to s\gamma$ rescattering and we have dropped out the tiny contributions proportional to CKM sector $V_{ub}V_{us}^*$.

In terms of the above Hamiltonian, the free quark decay amplitude for $b \to s\ell^+\ell^-$ in the SM can be derived as:

$$\mathcal{M}(b \rightarrow s\ell^{+}\ell^{-}) = -\frac{G_{F}\alpha}{\sqrt{2}\pi} V_{tb} V_{ts}^{*} \bigg\{ C_{9}^{SM}(\bar{s}\gamma_{\mu}P_{L}b)(\bar{l}\gamma^{\mu}l) + C_{10}^{SM}(\bar{s}\gamma_{\mu}P_{L}b)(\bar{l}\gamma^{\mu}\gamma_{5}l) - 2m_{b}C_{7}^{SM}(\bar{s}i\sigma_{\mu\nu}\frac{q^{\nu}}{q^{2}}P_{R}b)(\bar{l}\gamma^{\mu}l) \bigg\},$$

$$(10)$$

where $q^2 = (p_{l^+} + p_{l^-})^2$ is the square of momentum transfer.

B. Universal Extra Dimension Model

Among different new physics models cooked during last 20 years or so, a special role is played by one with universal extra dimensions (UED). In this model all SM fields are allowed to propagate in all available dimensions. The economy of UED model is that there is only one additional parameter to that of SM which is the radius R of the compactified extra dimension. Now above the compactification scale 1/R a given UED model becomes a higher dimensional field theory whose equivalent description in four dimensions consists of SM fields and the towers of Kaluza-Klein (KK) modes having no partner in the SM. A simplest model of this type was proposed by Appelquist, Cheng and Dobrescu (ACD) [80]. In this model, all the masses of the KK particles and their interactions with SM particles and also among themselves are described in terms of the inverse of compactification radius R and the parameters of the SM [81, 82].

The ACD model belongs to the class of Minimal Flavor Violating models where the effects beyond SM are only encoded in the Wilson coefficients of the effective Hamiltonian without changing the operator basis of SM. Wilson coefficients contributing in the calculation of $b \to s\ell^+\ell^-$ i.e. C_7 , C_9 and C_{10} get modified due to the KK excitation inducing a dependence on the compactification radius R. As the value of the compactification radius R becomes smaller or in other words the value of 1/R, becomes larger we can recover the Standard Model phenomenology because the massive KK states started to decouple. As a general expression, the Wilson coefficients are represented by periodic functions $F(x_t, 1/R)$ generalizing their SM analogues $F_0(x_t)$:

$$F(x_t, 1/R) = F_0(x_t) + \sum_{n=1}^{\infty} F(x_t, x_n)$$
(11)

with $x_t = \frac{m_t^2}{M_w^2}$, $x_n = \frac{m_n^2}{M_w^2}$ and $m_n = \frac{n}{R}$. The remarkable feature of above equation is that the summation over the KK contribution is finite at the leading order (LO) in all the cases as a consequence of generalized GIM mechanism [81, 82]. As $R \to 0$, $F(x_t, 1/R) \to F_0(x_t)$ which is the SM result. Now if we take 1/R to be few hundred GeV, the values of the Wilson coefficients differ considerable from their corresponding SM values, where the most pronounced effects comes in the C_7 . It is therefore expected that the various physical observables differ significantly from the SM results for certain range of compactification radius R.

Thus the effective Hamiltonian for $b \to s\ell^+\ell^-$ transition in UED model is given by

$$\mathcal{H}_{eff}^{UED}(b \rightarrow s\ell^{+}\ell^{-}) = -\frac{G_{F}\alpha}{\sqrt{2\pi}} V_{tb} V_{ts}^{*} \bigg\{ C_{9}^{UED}(\bar{s}\gamma_{\mu}P_{L}b)(\bar{l}\gamma^{\mu}l) + C_{10}^{UED}(\bar{s}\gamma_{\mu}P_{L}b)(\bar{l}\gamma^{\mu}\gamma_{5}l) - 2m_{b}C_{7}^{UED}(\bar{s}i\sigma_{\mu\nu}\frac{q^{\nu}}{q^{2}}P_{R}b)(\bar{l}\gamma^{\mu}l) \bigg\},$$

$$(12)$$

where the explicit expressions of various Wilson coefficients are given in Refs. [81, 82]. Using this Hamiltonian the free quark decay amplitude becomes

$$\mathcal{M}(b \rightarrow s\ell^{+}\ell^{-}) = -\frac{G_{F}\alpha}{\sqrt{2}\pi} V_{tb} V_{ts}^{*} \bigg\{ C_{9}^{UED}(\bar{s}\gamma_{\mu}P_{L}b)(\bar{l}\gamma^{\mu}l) + C_{10}^{UED}(\bar{s}\gamma_{\mu}P_{L}b)(\bar{l}\gamma^{\mu}\gamma_{5}l) - 2m_{b}C_{7}^{UED}(\bar{s}i\sigma_{\mu\nu}\frac{q^{\nu}}{q^{2}}P_{R}b)(\bar{l}\gamma^{\mu}l) \bigg\}.$$
(13)

C. Family Non-universal Z' Model

A family non-universal Z' boson could be derived naturally in many extensions of the SM and the one easiest way to get it is to include an additional U'(1) gauge symmetry. This has been formulated in detail by Langacker and Plümacher [84]. Now in a family non-universal Z' model, FCNC transitions $b \to s\ell^+\ell^-$ could be induced at tree level because of the non-diagonal chiral coupling matrix. Taken to be for granted, the couplings of right handed quark flavors with Z' boson are diagonal and ignoring Z - Z' mixing, the effective Hamiltonian for $b \to s\ell^+\ell^-$ can be written as [85]

$$\mathcal{H}_{eff}^{Z'}(b \to s\ell^+\ell^-) = -\frac{2G_F}{\sqrt{2}} V_{tb}^* V_{ts} B_{sb} \left[\frac{4\pi}{\alpha V_{tb}^* V_{ts}} S_{\ell\ell}^L \bar{\ell} \gamma^\mu \left(1 - \gamma^5\right) \ell - \frac{4\pi S_{\ell\ell}^R}{\alpha V_{tb}^* V_{ts}} \bar{\ell} \gamma^\mu \left(1 + \gamma^5\right) \ell \right] \bar{s} \gamma_\mu \left(1 - \gamma^5\right) b + h.c.$$
(14)

where $S_{\ell\ell}^L$ and $S_{\ell\ell}^R$ represents the coupling of Z' boson with the left and right handed leptons, respectively and B_{sb} corresponds to the off diagonal left handed coupling of quarks with new Z' boson in a case when the weak phase ϕ_{sb} is neglected. In a situation when the weak phase is introduced in the off diagonal coupling then this coupling reads as $B_{sb} = |B_{sb}|e^{-i\phi_{sb}}$. One can reformulate the effective Hamiltonian given in Eq.(14) as

$$H_{eff}^{Z'}(b \to s\ell^+\ell^-) = -\frac{4G_F}{\sqrt{2}}V_{tb}^*V_{ts}\left[\bar{C}_9^{Z'}O_9 + \bar{C}_{10}^{Z'}O_{10}\right] + h.c.$$

where

$$\bar{C}_{9}^{Z'} = \frac{4\pi e^{-i\phi_{sb}}}{\alpha V_{tb}^* V_{ts}} \Re[B_{sb}] S_{LL}$$

$$\bar{C}_{10}^{Z'} = \frac{4\pi e^{-i\phi_{sb}}}{\alpha V_{tb}^* V_{ts}} \Re[B_{sb}] D_{LL}$$
(15)

with

$$S_{LL} = S_{\ell\ell}^L + S_{\ell\ell}^R$$
$$D_{LL} = S_{\ell\ell}^L - S_{\ell\ell}^R$$

Hence the contribution of Z' boson leads to the modification the Wilson coefficients C_9 and C_{10} which now take the form

$$C_9^{Z'} = C_9^{SM} + \bar{C}_9^{Z'}$$
$$C_{10}^{Z'} = C_{10}^{SM} + \bar{C}_{10}^{Z'}$$

while the Wilson coefficient C_7 remains unchanged.

III. MATRIX ELEMENTS AND FORM FACTORS IN LIGHT CONE SUM RULES

In order to calculate the decay amplitudes for $B_s \to \phi \ell^+ \ell^-$ at hadron level, we have to sandwich the free quark amplitudes between the initial and final meson states. Consequently, the following four hadronic matrix elements

$$\langle \phi(k,\varepsilon) | \bar{s}\gamma_{\mu} b | B_{s}(p) \rangle , \quad \langle \phi(k,\varepsilon) | \bar{s}\gamma_{\mu}\gamma_{5} b | B_{s}(p) \rangle , \langle \phi(k,\varepsilon) | \bar{s}\sigma_{\mu\nu} b | B_{s}(p) \rangle , \quad \langle \phi(k,\varepsilon) | \bar{s}\sigma_{\mu\nu}\gamma_{5} b | B_{s}(p) \rangle ,$$

$$(16)$$

need to be computed. The above matrix elements can be parameterized in terms of the form factors as

$$\langle \phi(k,\varepsilon) | \bar{s}\gamma_{\mu} b | B_{s}(p) \rangle = \varepsilon_{\mu\nu\rho\sigma} \varepsilon^{*\nu} p^{\rho} k^{\sigma} \frac{2V(q^{2})}{M_{B_{s}} + M_{\phi}}, \qquad (17)$$

$$\langle \phi(k,\varepsilon) | \bar{s}\gamma_{\mu}\gamma_{5}b | B_{s}(p) \rangle = i\varepsilon_{\mu}^{*} \left(M_{B_{s}} + M_{\phi} \right) A_{1} \left(q^{2} \right) - i(p+k)_{\mu} (\varepsilon^{*} \cdot q) \frac{A_{2} \left(q^{2} \right)}{M_{B_{s}} + M_{\phi}} - iq_{\mu} (\varepsilon^{*} \cdot q) \frac{2M_{\phi}}{q^{2}} \left[A_{3} \left(q^{2} \right) - A_{0} \left(q^{2} \right) \right],$$
(18)

$$\langle \phi(k,\varepsilon) | \bar{s}\sigma_{\mu\nu}q^{\nu}b | B_s(p) \rangle = i\varepsilon_{\mu\nu\rho\sigma}\varepsilon^{*\nu}p^{\rho}k^{\sigma}2T_1(q^2), \qquad (19)$$

$$\langle \phi(k,\varepsilon) | \bar{s}\sigma_{\mu\nu}\gamma_5 q^{\nu}b | B_s(p) \rangle = T_2(q^2) [\varepsilon^*_{\mu}(M^2_{B_s} - M^2_{\phi}) - (p+k)_{\mu}(\varepsilon^* \cdot q)]$$

$$(\varepsilon,\varepsilon) |s\sigma_{\mu\nu}\gamma_5 q^{\nu}b|B_s(p)\rangle = T_2(q^2) [\varepsilon^*_{\mu} (M^2_{B_s} - M^2_{\phi}) - (p+k)_{\mu}(\varepsilon^* \cdot q)]$$

$$+T_3(q^2)(\varepsilon^* \cdot q) \left[q_{\mu} - \frac{q^2}{M_{B_s}^2 - M_{\phi}^2} (p+k)_{\mu} \right], \qquad (20)$$

where all the form factors A_i and T_i are functions of the square of momentum transfer $q^2 = (p-k)^2$ and $\varepsilon^{*\nu}$ is the polarization of the final state vector meson (ϕ) . The form factors A_i and T_i appearing in the above equations are not independent but can be related to each other with the help of equation of motion. The various relationship between the form factors are [52]

$$A_{3}(q^{2}) = \frac{M_{B_{s}} + M_{\phi}}{2M_{\phi}} A_{1}(q^{2}) - \frac{M_{B_{s}} - M_{\phi}}{2M_{\phi}} A_{2}(q^{2})$$

$$A_{3}(0) = A_{0}(0), T_{1}(0) = T_{2}(0).$$
(21)

The form factors for $B_s \to \phi$ transition are the non-perturbative quantities and are needed to be calculated using different approaches (both perturbative and non-perturbative) like Lattice QCD, QCD sum rules, Light Cone sum rules, etc. Here, we will consider the form factors calculated by using the Light Cone Sum Rules approach by Ball and Braun [53]. The form factors V, A_0 and T_1 are parameterized by

$$F(q^2) = \frac{r_1}{1 - q^2/m_R^2} + \frac{r_2}{1 - q^2/m_{fit}^2}$$
(22)

While the form factors A_2 and \tilde{T}_3 are parameterized as follows,

$$F(q^2) = \frac{r_1}{1 - q^2/m^2} + \frac{r_2}{(1 - q^2/m^2)^2}$$
(23)

The fit formula for A_1 and T_2 is

$$F(q^2) = \frac{r_2}{1 - q^2/m_{fit}^2} \tag{24}$$

The form factor T_3 can be obtained through the relation

$$T_3(q^2) = \frac{M_{B_s}^2 - M_{\phi}^2}{q^2} [\tilde{T}_3(q^2 - T_2(q^2))]$$

where the values of different parameters are summarized in Table I.

From Eqs. (17 - 20) it is straightforward to find the matrix elements for $B_s \to \phi \ell^+ \ell^-$ as follows:

$$\mathcal{M} = -\frac{G_F \alpha}{2\sqrt{2}\pi M_{B_s}^2} V_{tb} V_{ts}^* \left[\mathcal{T}_{\mu}^1 \left(\bar{l} \gamma^{\mu} l \right) + \mathcal{T}_{\mu}^2 \left(\bar{l} \gamma^{\mu} \gamma_5 l \right) + \mathcal{T}^3 \left(\bar{l} l \right) \right]$$
(25)

$F(q^2)$	F(0)	r_1	m_R^2	r_2	m_{fit}^2
$A_1(q^2)$	0.311	_	—	0.308	36.54
$A_2(q^2)$	0.234	-0.054	_	0.288	48.94
$A_0(q^2)$	0.474	3.310	5.28^{2}	-2.835	31.57
$V(q^2)$	0.434	1.484	5.32^{2}	-1.049	39.52
$T_1(q^2)$	0.349	1.303	5.32^{2}	-0.954	38.28
$T_2(q^2)$	0.349	_	—	0.349	37.21
$\tilde{T}_3(q^2)$	0.349	0.027	—	0.321	45.56

TABLE I: Fit parameters for $B_s \to \phi$ transition form factors. F(0) denotes the value of form factors at $q^2 = 0$ Eq. (22)[53]. The theoretical uncertainty estimated is around 15%.

where

$$\mathcal{T}^{1}_{\mu} = f_{1}(q^{2})\epsilon_{\mu\nu\alpha\beta}\varepsilon^{*\nu}p^{\alpha}k^{\beta} - if_{2}(q^{2})\varepsilon^{*}_{\mu} + if_{3}(q^{2})(\varepsilon^{*} \cdot p)P_{\mu}$$

$$\tag{26}$$

$$\mathcal{T}^2_{\mu} = f_4(q^2)\epsilon_{\mu\nu\alpha\beta}\varepsilon^{*\nu}p^{\alpha}k^{\beta} - if_5(q^2)\varepsilon^*_{\mu} + if_6(q^2)(\varepsilon^* \cdot p)P_{\mu} + if_7(q^2)(\varepsilon^* \cdot p)P_{\mu}$$
(27)

with $P_{\mu} = p_{\mu} + k_{\mu}$. The auxiliary functions appearing in above equation can be written as

$$f_1(q^2) = 4\widetilde{C}_7(\frac{m_b + m_s}{q^2})T_1(q^2) + \widetilde{C}_9 \frac{2V(q^2)}{M_{B_s} + M_\phi}$$
(28)

$$f_{2}(q^{2}) = 2\widetilde{C}_{7}\left(\frac{m_{b} - m_{s}}{q^{2}}\right)T_{2}(q^{2})\left(M_{B_{s}}^{2} - M_{\phi}^{2}\right) + \widehat{C}_{9}A_{1}(q^{2})\left(M_{B_{s}} + M_{\phi}\right)$$
(29)

$$f_{3}(q^{2}) = 4\widetilde{C}_{7}\left(\frac{m_{b} - m_{s}}{q^{2}}\right) \left(T_{2}(q^{2}) + q^{2} \frac{T_{3}(q^{2})}{\left(M_{B_{s}}^{2} - M_{\phi}^{2}\right)}\right) + \widehat{C}_{9} \frac{A_{+}(q^{2})}{M_{-} + M_{-}}$$
(30)

$$M_{B_s} + M_{\phi}$$

$$f_4(q^2) = \tilde{C}_{10} \frac{2V(q^2)}{2V(q^2)}$$
(31)

$$f_{5}(q^{2}) = 2\tilde{C}_{10}A_{0}(q^{2}) (M_{B_{s}} + M_{\phi})$$
(32)

$$f_6(q^2) = 2\tilde{C}_{10} \frac{A_1(q^2)}{M_{B_2} + M_{\phi}}$$
(33)

$$f_7(q^2) = 4\tilde{C}_{10} \frac{A_2(q^2)}{M_{B_s} + M_\phi}$$
(34)

Here the Wilson coefficients \tilde{C}_i will be different for different models and these are gathered in Table II.

TABLE II: Wilson coefficients corresponding to the models under discussion here.

	SM UED	Z'model
\widetilde{C}_7	$C_7^{SM} C_7^{UED}$	C_7^{SM}
\widetilde{C}_9	$C_9^{SM} \ C_9^{UED}$	$C_9^{Z'}$
\widetilde{C}_{10}	$C_{10}^{SM} \ C_{10}^{UED}$	$C_{10}^{Z'}$

IV. FORMULA FOR OBSERVABLES

In this section we will present the calculations of the physical observables such as the branching ratios \mathcal{BR} , the forward-backward asymmetries \mathcal{A}_{FB} , the single lepton polarization asymmetries $P_{L,N,T}$, the double lepton polarization

asymmetries P_{ij} (i, j = L, N, T), the helicity fractions $f_{L,T}$ of the ϕ meson and the polarized and un-polarized CP asymmetries of the final state lepton in $B_s \to \phi \ell^+ \ell^-$ decay.

A. The Differential Decay Rate

In the rest frame of B_s meson the differential decay width of $B_s \to \phi \ell^+ \ell^-$ can be written as

$$\frac{d\Gamma(B_s \to \phi \ell^+ \ell^-)}{dq^2} = \frac{1}{(2\pi)^3} \frac{1}{32M_{B_s}^3} \int_{-u(q^2)}^{+u(q^2)} du \left|\mathcal{M}\right|^2 \tag{35}$$

where

$$q^2 = (p_+ + p_-)^2 \tag{36}$$

$$u = (p - p_{-})^{2} - (p - p_{+})^{2}.$$
(37)

The limits on q^2 and u are

$$4m_l^2 \le q^2 \le (M_{B_s} - M_\phi)^2 \tag{38}$$

$$-u(q^2) \leq u \leq u(q^2) \tag{39}$$

with

$$u(q^2) = \sqrt{\lambda \left(1 - \frac{4m_l^2}{q^2}\right)} \tag{40}$$

and

$$\lambda \equiv \lambda(M_{B_s}^2, M_{\phi}^2, q^2) = M_{B_s}^4 + M_{\phi}^4 + q^4 - 2M_{B_s}^2 M_{\phi}^2 - 2M_{\phi}^2 q^2 - 2q^2 M_{B_s}^2$$
(41)

In above expressions, m_l corresponds to the mass of the lepton which for our case can be μ or τ . The total decay rate for the decay $B_s \to \phi \ell^+ \ell^-$ can take the form

$$\frac{d\Gamma}{dq^2} = \frac{G_F^2 \left| V_{tb} V_{ts}^* \right|^2 \alpha^2}{2^{11} \pi^5 3 M_{B_s}^3 M_{\phi}^2 q^2} u(q^2) \times \mathcal{A}\left(q^2\right)$$
(42)

The function $u(q^2)$ is defined in Eq. (40) and $\mathcal{A}(q^2)$ is given by

$$\mathcal{A}(q^{2}) = 8M_{\phi}^{2}q^{2}\lambda\left\{\left(2m_{l}^{2}+q^{2}\right)\left|f_{1}(q^{2})\right|^{2}-\left(4m_{l}^{2}-q^{2}\right)\left|f_{4}(q^{2})\right|^{2}\right\}+4M_{\phi}^{2}q^{2}\left\{\left(2m_{l}^{2}+q^{2}\right)\right\}$$

$$\times\left(3\left|f_{2}(q^{2})\right|^{2}-\lambda\left|f_{3}(q^{2})\right|^{2}\right)-\left(4m_{l}^{2}-q^{2}\right)\left(3\left|f_{5}(q^{2})\right|^{2}-\lambda\left|f_{6}(q^{2})\right|^{2}\right)\right\}$$

$$+\lambda(2m_{l}^{2}+q^{2})\left|f_{2}(q^{2})+\left(M_{B_{s}}^{2}-M_{\phi}^{2}-q^{2}\right)f_{3}(q^{2})\right|^{2}+24m_{l}^{2}M_{\phi}^{2}\lambda\left|f_{7}(q^{2})\right|^{2}$$

$$-\left(4m_{l}^{2}-q^{2}\right)\left|f_{5}(q^{2})+\left(M_{B_{s}}^{2}-M_{\phi}^{2}-q^{2}\right)f_{6}(q^{2})\right|^{2}$$

$$-12m_{l}^{2}q^{2}\left[\Re(f_{5}f_{7}^{*})-\Re(f_{6}f_{7}^{*})\right].$$
(43)

B. Forward-Backward Asymmetries

The differential forward-backward asymmetry \mathcal{A}_{FB} of final state lepton for the said decay can be written as

$$\frac{d\mathcal{A}_{FB}(s)}{dq^2} = \int_0^1 \frac{d^2\Gamma}{dq^2 d\cos\theta} d\cos\theta - \int_{-1}^0 \frac{d^2\Gamma}{dq^2 d\cos\theta} d\cos\theta \tag{44}$$

From experimental point of view the normalized forward-backward asymmetry is more useful, defined as

$$\mathcal{A}_{FB} = \frac{\int_0^1 \frac{d^2 \Gamma}{dq^2 d \cos \theta} d \cos \theta - \int_{-1}^0 \frac{d^2 \Gamma}{dq^2 d \cos \theta} d \cos \theta}{\int_{-1}^1 \frac{d^2 \Gamma}{dq^2 d \cos \theta} d \cos \theta}$$

The normalized \mathcal{A}_{FB} for $B_s \to \phi \ell^+ \ell^-$ can be obtained from Eq. (35), as

$$\mathcal{A}_{FB} = -\frac{1}{d\Gamma/dq^2} \frac{G_F^2 \alpha^2}{2^{11} \pi^5 M_{B_s}^3} |V_{tb} V_{ts}^*|^2 q^2 u(q^2) \times \left\{ 4Re[f_2^* f_4 + f_1^* f_5] \right\}$$
(45)

where $d\Gamma/dq^2$ is given in Eq. (42). Confining ourself to the SM, the above expression of the FB asymmetry in terms of the Wilson coefficients becomes

$$\mathcal{A}_{FB} = -\frac{1}{d\Gamma/dq^2} \frac{G_F^2 \alpha^2}{2^8 \pi^5 M_{B_s}^3} |V_{tb} V_{ts}^*|^2 q^2 u(q^2) \times C_{10}$$

$$\left\{ \Re \left(C_9^{eff} \right) V\left(q^2\right) A_1\left(q^2\right) \frac{m_b}{q^2} C_7^{eff} \left(V\left(q^2\right) T_2\left(q^2\right) \left(M_{B_s} - M_\phi\right) + A_1\left(q^2\right) T_1\left(q^2\right) \left(M_{B_s} + M_\phi\right) \right) \right\}$$

$$(46)$$

which in agreement with the one obtained for $B \to K^* l^+ l^-$ decay in [13].

C. Lepton Polarization Asymmetries

In the rest frame of the lepton ℓ^- , the unit vectors along longitudinal, normal and transversal component of the ℓ^- can be defined as [86–88]:

$$s_L^{-\mu} = (0, \vec{e}_L) = \left(0, \frac{\vec{p}_-}{|\vec{p}_-|}\right),$$
(47a)

$$s_N^{-\mu} = (0, \vec{e}_N) = \left(0, \frac{\vec{k} \times \vec{p}_-}{\left|\vec{k} \times \vec{p}_-\right|}\right), \tag{47b}$$

$$s_T^{-\mu} = (0, \vec{e}_T) = (0, \vec{e}_N \times \vec{e}_L),$$
(47c)

where \vec{p}_{-} and \vec{k} are the three-momenta of the lepton ℓ^{-} and ϕ meson respectively in the center mass (c.m.) frame of $\ell^{+}\ell^{-}$ system. Lorentz transformation is used to boost the longitudinal component of the lepton polarization to the c.m. frame of the lepton pair as

$$(s_L^{-\mu})_{CM} = \left(\frac{|\vec{p}_-|}{m_l}, \frac{E\vec{p}_-}{m_l\,|\vec{p}_-|}\right)$$
(48)

where E and m_l are the energy and mass of the lepton. The normal and transverse components remain unchanged under the Lorentz boost. The longitudinal (P_L) , normal (P_N) and transverse (P_T) polarizations of lepton can be defined as:

$$P_i^{(\mp)}(q^2) = \frac{\frac{d\Gamma}{dq^2}(\vec{\xi}^{\mp} = \vec{e_i}^{\,\mp}) - \frac{d\Gamma}{dq^2}(\vec{\xi}^{\mp} = -\vec{e_i}^{\,\mp})}{\frac{d\Gamma}{dq^2}(\vec{\xi}^{\mp} = \vec{e_i}^{\,\mp}) + \frac{d\Gamma}{dq^2}(\vec{\xi}^{\mp} = -\vec{e_i}^{\,\mp})}$$
(49)

where i = L, N, T and $\vec{\xi}^{\mp}$ is the spin direction along the leptons ℓ^{\mp} . The differential decay rate for polarized lepton ℓ^{\mp} in $B_s \to \phi \ell^+ \ell^-$ decay along any spin direction $\vec{\xi}^{\mp}$ is related to the unpolarized decay rate (42) with the following relation

$$\frac{d\Gamma(\vec{\xi^{\mp}})}{dq^2} = \frac{1}{2} \left(\frac{d\Gamma}{dq^2} \right) \left[1 + \left(P_L^{\mp} \vec{e}_L^{\mp} + P_N^{\mp} \vec{e}_N^{\mp} + P_T^{\mp} \vec{e}_T^{\mp} \right) \cdot \vec{\xi^{\mp}} \right].$$
(50)

The expressions of the longitudinal, normal and transverse lepton polarizations can be written as

$$P_{L}(q^{2}) \propto \frac{4\lambda}{3M_{\phi}^{2}} \sqrt{\frac{q^{2} - 4m_{l}^{2}}{q^{2}}} \times \left\{ 2\Re(f_{2}f_{5}^{*}) + \lambda\Re(f_{3}f_{6}^{*}) + 4\sqrt{q^{2}}\Re(f_{1}f_{4}^{*}) \left(1 + \frac{12q^{2}M_{\phi}^{2}}{\lambda}\right) + \left(-M_{B_{s}}^{2} + M_{\phi}^{2} + q^{2}\right) \left[\Re(f_{3}f_{5}^{*}) + \Re(f_{2}f_{6}^{*})\right] \right\}$$

$$(51)$$

$$P_{N}(q^{2}) \propto -\frac{m_{l}\pi}{M_{\phi}^{2}} \sqrt{\frac{\lambda}{q^{2}}} \times \left\{ \lambda q^{2} \Re(f_{3}f_{7}^{*}) - \lambda (M_{B_{s}}^{2} - M_{\phi}^{2}) \Re(f_{3}f_{6}^{*}) + \lambda \Re(f_{3}f_{5}^{*}) + \left(M_{B_{s}}^{2} - M_{\phi}^{2} - q^{2}\right) \left[q^{2} \Re(f_{2}f_{7}^{*}) + (M_{B_{s}}^{2} - M_{\phi}^{2}) \Re(f_{2}f_{5}^{*})\right] + 8q^{2} M_{\phi}^{2} \Re(f_{1}f_{2}^{*}) \right\}$$

$$(52)$$

$$P_T(q^2) \propto i \frac{m_l \pi \sqrt{\left(q^2 - \frac{4m_l^2}{q^2}\right)\lambda}}{M_{\phi}^2} \bigg\{ M_{\phi} \left[4\Im(f_2 f_4^*) + 4\Im(f_1 f_5^*) + 3\Im(f_5 f_6^*)\right] \\ - \lambda\Im(f_6 f_7^*) + \left(-M_{B_s}^2 + M_{\phi}^2 + q^2\right)\Im(f_7 f_5^*) - q^2\Im(f_5 f_6^*)\bigg\}$$
(53)

where f_1, f_2, \dots, f_7 are the auxiliary functions defined above. Here we have dropped out the constant factors which are however understood.

D. Double Lepton Polarization Asymmetries

To calculate the double-polarization asymmetries, we consider the polarizations of both lepton and anti-lepton, simultaneously and introduce the following spin projection operators for the lepton ℓ^- and the anti-lepton $\ell^+[91]$:

$$\Lambda_1 = \frac{1}{2} \left(1 + \gamma_5 \boldsymbol{\sharp}_i^- \right)$$

$$\Lambda_2 = \frac{1}{2} \left(1 + \gamma_5 \boldsymbol{\sharp}_i^+ \right)$$
(54)

where i = L, T and N corresponds to the longitudinal, transverse and normal lepton polarizations, respectively. In the rest frame of the lepton-anti-lepton one can define the following set of orthogonal vectors s^{μ} :

$$s_{L}^{-\mu} = (0, \vec{e}_{L}) = \left(0, \frac{\vec{p}_{-}}{|\vec{p}_{-}|}\right),$$

$$s_{N}^{-\mu} = (0, \vec{e}_{N}) = \left(0, \frac{\vec{k} \times \vec{p}_{-}}{|\vec{k} \times \vec{p}_{-}|}\right),$$

$$s_{T}^{-\mu} = (0, \vec{e}_{T}) = (0, \vec{e}_{N} \times \vec{e}_{L}),$$

$$s_{L}^{+\mu} = (0, \vec{e}_{L}^{+}) = \left(0, \frac{\vec{p}_{+}}{|\vec{p}_{+}|}\right),$$

$$s_{N}^{+\mu} = (0, \vec{e}_{N}^{+}) = \left(0, \frac{\vec{k} \times \vec{p}_{+}}{|\vec{k} \times \vec{p}_{+}|}\right),$$

$$s_{T}^{+\mu} = (0, \vec{e}_{T}^{+}) = (0, \vec{e}_{N} \times \vec{e}_{L}).$$
(55)

Just like the single lepton polarization, through Lorentz transformations we can boost the longitudinal component in the CM frame of $\ell^-\ell^+$ as

$$(s_{L}^{-\mu})_{CM} = \left(\frac{|\vec{p}_{-}|}{m_{l}}, \frac{E\vec{p}_{-}}{m_{l}|\vec{p}_{-}|}\right) (s_{L}^{+\mu})_{CM} = \left(\frac{|\vec{p}_{+}|}{m_{l}}, -\frac{E\vec{p}_{+}}{m_{l}|\vec{p}_{+}|}\right)$$
(56)

The normal and transverse component remains the same under Lorentz boost. We now define the double lepton polarization asymmetries as

$$P_{ij}(q^2) = \frac{\left(\frac{d\Gamma}{dq^2}\left(\vec{s}_i^-, \vec{s}_i^+\right) - \frac{d\Gamma}{dq^2}\left(-\vec{s}_i^-, \vec{s}_i^+\right)\right) - \left(\frac{d\Gamma}{dq^2}\left(\vec{s}_i^-, -\vec{s}_i^+\right) - \frac{d\Gamma}{dq^2}\left(-\vec{s}_i^-, -\vec{s}_i^+\right)\right)}{\left(\frac{d\Gamma}{dq^2}\left(\vec{s}_i^-, \vec{s}_i^+\right) - \frac{d\Gamma}{dq^2}\left(-\vec{s}_i^-, \vec{s}_i^+\right)\right) + \left(\frac{d\Gamma}{dq^2}\left(\vec{s}_i^-, -\vec{s}_i^+\right) - \frac{d\Gamma}{dq^2}\left(-\vec{s}_i^-, -\vec{s}_i^+\right)\right)}\right)}$$
(57)

where the subscripts i and j corresponds to the lepton and anti-lepton polarizations, respectively. Using these definitions the various double lepton polarization asymmetries as a function of q^2 can be written as

$$P_{LL}(q^{2}) \propto \frac{1}{3m_{l}^{2}} \{4 |f_{1}|^{2} \left(8m_{l}^{4}\lambda - q^{2}\mathcal{U}_{2}\right) + 4 |f_{4}|^{2}\mathcal{U}_{1} + \frac{1}{M_{\phi}^{2}} [24m_{l}^{4}\lambda \left(M_{B_{s}}^{2} - M_{\phi}^{2}\right) \left(f_{6}f_{7}^{*} + f_{7}f_{6}^{*}\right) \\ -12m_{l}^{4}\lambda \left(2f_{5}f_{7}^{*} + 2f_{7}f_{5}^{*}\right) + 12 |f_{7}|^{2} m_{l}^{4}q^{2}\lambda + \left(\left(q^{2} - M_{B_{s}}^{2} + M_{\phi}^{2}\right) \left(\frac{4m_{l}^{4}\lambda}{q^{2}} - 6m_{l}^{2}\lambda + \mathcal{U}_{2}\right)\right) \left(f_{1}f_{2}^{*} + f_{2}f_{1}^{*}\right) \\ + |f_{2}|^{2} \left(\frac{4m_{l}^{4}\lambda}{q^{2}} \left(\lambda + 12M_{\phi}^{2}q^{2}\right) - 3m_{l}^{2} \left(2\lambda + 8M_{\phi}^{2}q^{2}\right) + \mathcal{U}_{2}\right) \\ - \frac{4m_{l}^{4}}{q^{2}}\mathcal{U}_{3}(f_{5}^{*}f_{6} + f_{6}^{*}f_{5}) + \lambda |f_{6}|^{2} \left(\frac{4m_{l}^{4}}{q^{2}}\mathcal{U}_{4} + 2m_{l}^{2}\lambda + \mathcal{U}_{2}\right) \\ + \lambda |f_{5}|^{2} \left(\frac{4m_{l}^{4}}{q^{2}} \left(6 \left(q^{2} - M_{B_{s}}^{2} + M_{\phi}^{2}\right)^{2} - \lambda\right) - 3m_{l}^{2} \left(6\lambda + 8M_{\phi}^{2}q^{2}\right) + q^{2}\mathcal{U}_{2})]\}$$

$$P_{LT} \propto \frac{1}{4M_{\phi}^{2}q^{2}}\pi\sqrt{\lambda}\sqrt{q^{2}-4m_{l}^{2}}\{8m_{l}M_{\phi}^{2}q^{2}\left(f_{2}^{*}f_{4}+f_{2}f_{4}^{*}\right)+2m_{l}\left(M_{B_{s}}^{2}q^{2}\left(f_{5}^{*}f_{7}+3f_{5}^{*}f_{6}\right)\right)$$

$$+M_{\phi}^{2}q^{2}\left(4f_{5}^{*}f_{1}-f_{5}^{*}f_{7}\right)-q^{4}\left(f_{5}^{*}f_{7}+f_{5}^{*}f_{6}\right)-2f_{5}^{*}f_{6}\left(M_{B_{s}}^{2}-M_{\phi}^{2}\right)^{2}$$

$$+2\left(M_{B_{s}}^{2}-M_{\phi}^{2}\right)\left(\left|f_{5}\right|^{2}-f_{5}f_{6}^{*}\left(M_{B_{s}}^{2}-M_{\phi}^{2}\right)\right)+q^{2}\left(f_{5}f_{6}^{*}\left(3M_{B_{s}}^{2}+M_{\phi}^{2}\right)-2\left|f_{5}\right|^{2}\right)-f_{5}f_{6}^{*}q^{4}\right)$$

$$+4m_{l}\lambda\left(q^{2}\left(f_{7}f_{6}^{*}+f_{6}f_{7}^{*}\right)+\left|f_{6}\right|^{2}\left(M_{B_{s}}^{2}-M_{\phi}^{2}\right)\right)\}$$
(59)

$$P_{LN} \propto -i \frac{1}{4M_{\phi}^2 \sqrt{q^2}} \pi \sqrt{\lambda} \{ 2m_l \left(M_B^2 - M_{\phi}^2 - q^2 \right) \left(q^2 f_2^* f_7 + f_2^* f_6 \left(M_B^2 - M_{\phi}^2 \right) - f_2^* f_5 \right) + 2m_l \lambda \left(f_3^* f_5 - f_3^* f_6 \left(M_B^2 - M_{\phi}^2 \right) - q^2 f_3^* f_7 \right) \}$$

$$(60)$$

$$P_{TL} \propto \frac{1}{4M_{\phi}^{2}q^{2}} \pi \sqrt{\lambda} \sqrt{q^{2} - 4m_{l}^{2}} \{4m_{l}\lambda \left(q^{2}(f_{6}^{*}f_{7} + f_{7}^{*}f_{6}) + |f_{7}|^{2} (M_{B_{s}}^{2} - M_{\phi}^{2})\right) - 8m_{l}M_{\phi}^{2}q^{2} (f_{4}^{*}f_{2} + f_{2}^{*}f_{4}) + 2m_{l}(q^{2} (M_{\phi}^{2} - M_{B_{s}}^{2}) f_{5}^{*}f_{7} + q^{2} (M_{\phi}^{2} + 3M_{B_{s}}^{2}) f_{5}^{*}f_{6} + q^{4} (f_{5}^{*}f_{7} - f_{5}^{*}f_{6}) - 2f_{5}^{*}f_{6} (M_{B_{s}}^{2} - M_{\phi}^{2})^{2} + q^{2}f_{5}^{*}f_{6} (3M_{B_{s}}^{2} + M_{\phi}^{2}) + 2q^{2}f_{5}^{*}f_{7}(M_{\phi}^{2} - M_{B_{s}}^{2}) - 2q^{2} |f_{5}|^{2} + q^{4}(2f_{5}f_{7}^{*} - f_{5}f_{6}^{*}) + 2(M_{B_{s}}^{2} - M_{\phi}^{2})(|f_{5}|^{2} + f_{5}f_{6}^{*}(M_{\phi}^{2} - M_{B_{s}}^{2})) - 4M_{\phi}^{2}q^{2}f_{1}f_{5}^{*}(2\pi m_{l}\sqrt{\lambda}\sqrt{q^{2} - 4m_{l}^{2}})\}$$

$$(61)$$

$$P_{TN} \propto i\{\frac{4}{3}q\sqrt{q^2 - 4m_l^2} \left(4\lambda - 3M_{B_s}^4 + 6M_B^2(M_{\phi}^2 + q^2) - 3(M_{\phi}^2 - q^2)^2\right) + \sqrt{q^2\lambda}u \left(f_1f_4^* + f_1^*f_4\right)\}$$
(62)

$$P_{TT} \propto \frac{1}{3M_{\phi}^{2}q^{2}} \{48 |f_{2}|^{2} m_{l}^{2}M_{\phi}^{2}q^{2} - 4m_{l}^{2} \left(5 |f_{5}|^{2} + (M_{B_{s}}^{2} - M_{\phi}^{2})(f_{3}f_{2}^{*} - 5f_{5}^{*}f_{6})\right) + (2 |f_{5}|^{2} + 12f_{5}f_{7}^{*}m_{l}^{2} + (M_{B_{s}}^{2} - M_{\phi}^{2})(f_{3}f_{2}^{*} - f_{6}f_{5}^{*}))$$

$$+ 4m_{l}^{2}(3 + f_{3}f_{2}^{*} + 8M_{\phi}^{2}(|f_{1}|^{2} + |f_{4}|^{2}) - 2f_{6}f_{5}^{*}) - 2 \left(3(M_{B_{s}}^{2} - M_{\phi}^{2})f_{6}f_{7}^{*} + 3(M_{B_{s}}^{2} + M_{\phi}^{2})|f_{6}|^{2}\right) + 6q^{2} \left(f_{7}f_{5}^{*} - 2f_{7}f_{6}^{*}(M_{B_{s}}^{2} - M_{\phi}^{2})\right) + 2q^{4}(f_{6}f_{5}^{*} - f_{3}f_{2}^{*} + 6m_{l}^{2}(|f_{6}|^{2} - |f_{7}|^{2}) + 4M_{\phi}^{2}(|f_{1}|^{2} - |f_{4}|^{2})) + 2\lambda(q^{2} - 2m_{l}^{2}) \left(|f_{2}|^{2} + f_{2}f_{3}^{*}(q^{2} - M_{B_{s}}^{2} + M_{\phi}^{2})\right) + 2\lambda^{2} |f_{6}|^{2} (q^{2} - 10m_{l}^{2})\}$$

$$(63)$$

$$P_{NN} \propto -\frac{1}{3M_{\phi}^{2}q^{2}} \{48 |f_{2}|^{2} m_{l}^{2} M_{\phi}^{2}q^{2} - 4m_{l}^{2} (M_{B_{s}}^{2} - M_{\phi}^{2})(|f_{5}|^{2} + (f_{3}f_{2}^{*} - f_{6}f_{5}^{*})) + (4m_{l}^{2} + M_{B}^{2})f_{6}f_{5}^{*} + 12m_{l}^{2}f_{5}f_{7}^{*} - |f_{5}|^{2} + 12m_{l}^{2} M_{B_{s}}^{2}(|f_{6}|^{2} - f_{6}f_{7}^{*}) + 4m_{l}^{2} M_{\phi}^{2} \left(4 |f_{1}|^{2} - 4 |f_{4}|^{2} + 3(f_{6}f_{7}^{*} + |f_{6}|^{2})\right) + f_{3}f_{2}^{*}(2m_{l}^{2} - M_{B_{s}}^{2} + M_{\phi}^{2}) + 6m_{l}^{2}q^{2}(f_{7}f_{5}^{*} - 2f_{7}f_{6}^{*}(M_{B_{s}}^{2} - M_{\phi}^{2})) + q^{2}(f_{3}f_{2}^{*} - f_{6}f_{5}^{*} - 6m_{l}^{2}(|f_{7}|^{2} + |f_{6}|^{2}) + 4(|f_{4}|^{2} - |f_{1}|^{2})) + \lambda(q^{2} + 2m_{l}^{2}) \left(|f_{2}|^{2} + f_{2}f_{3}^{*}(q^{2} - M_{B_{s}}^{2} + M_{\phi}^{2}) + 2\lambda^{2} |f_{6}|^{2}\right)\}$$

$$(64)$$

with

$$\begin{aligned} \mathcal{U}_{1} &= m_{l}^{2}q^{2} \left(6M_{B_{s}}^{2} \left(M_{\phi}^{2} + q^{2} \right) - 3 \left(M_{\phi}^{2} - q^{2} \right)^{2} - 3M_{B_{s}}^{4} - 5\lambda \right) + q^{2}\mathcal{U}_{\epsilon} \\ \mathcal{U}_{2} &= \lambda q^{2} - \sqrt{q^{2} \left(q^{2} - 4m_{l}^{2} \right)} u\sqrt{\lambda} \\ \mathcal{U}_{3} &= 6 \left(M_{B_{s}}^{6} - M_{\phi}^{6} \right) + 9M_{\phi}^{4}q^{2} - 3q^{6} - 3M_{B_{s}}^{4} \left(6M_{\phi}^{2} + 5q^{2} \right) + M_{B_{s}}^{2} \left(18M_{\phi}^{4} + 6q^{2}M_{\phi}^{2} + 12q^{4} - \lambda \right) \\ &+ \lambda \left(M_{B_{s}}^{2} + M_{\phi}^{2} \right) + q^{2} \left(M_{B_{s}}^{2} - M_{\phi}^{2} - q^{2} \right) \mathcal{U}_{2} \\ \mathcal{U}_{4} &= 6 \left(M_{B_{s}}^{2} - M_{\phi}^{2} \right)^{2} - 6q^{2} \left(M_{B_{s}}^{2} + M_{\phi}^{2} \right) + 3q^{4} - \lambda \end{aligned}$$

and u and λ are defined in Eqs. (40) and (41), respectively.

Just to add few words about the lepton polarization asymmetry: we have seen that the expressions of various double lepton polarization asymmetries are function of the q^2 and of the parameters of NP models. From experimental point of view, it will be more interesting if we can eliminate the dependency on one parameter and this we can easily do by performing integration on q^2 . This will give us the average lepton polarization asymmetry and it is defined as:

$$\langle P_{ij} \rangle = \frac{\int P_{ij} \frac{dB}{dq^2} dq^2}{\int \int \frac{dB}{dq^2} dq^2}$$
(65)

E. Helicity Fractions of ϕ in $B_s \to \phi \ell^+ \ell^-$

We now discuss helicity fractions of ϕ in $B_s \to \phi \ell^+ \ell^-$ which are interesting variable and are as such independent of the uncertainties arising due to form factors and other input parameters. The final state meson helicity fractions were already discussed in literature for $B \to K^*(K_1) \ell^+ \ell^-$ decays [89, 90]. The explicit expression of the decay rate for $B_s^- \to \phi \ell^+ \ell^-$ decay can be written in terms of longitudinal Γ_L and

transverse components Γ_T as

$$\frac{d\Gamma(q^2)}{dq^2} = \frac{d\Gamma_L(q^2)}{dq^2} + \frac{d\Gamma_T(q^2)}{dq^2} \tag{66}$$

where

$$\frac{d\Gamma_T(q^2)}{dq^2} = \frac{d\Gamma_+(q^2)}{dq^2} + \frac{d\Gamma_-(q^2)}{dq^2}$$

and

$$\frac{d\Gamma_L(q^2)}{dq^2} = \frac{G_F^2 |V_{tb}V_{ts}^*|^2 \alpha^2}{2^{11}\pi^5} \frac{u(q^2)}{M_{B_2}^3} \times \frac{1}{3} \mathcal{A}_L$$
(67)

$$\frac{d\Gamma_{\pm}(q^2)}{dq^2} = \frac{G_F^2 |V_{tb}V_{ts}^*|^2 \alpha^2}{2^{11}\pi^5} \frac{u(q^2)}{M_{B_s}^3} \times \frac{4}{3} \mathcal{A}_{\pm}.$$
(68)

The different functions appearing in Eqs. (67) and (68) can be expressed in terms of auxiliary functions (cf. Eqs. (28-34)) as

$$\mathcal{A}_{L} = \frac{1}{q^{2}M_{\phi}^{2}} \left[24 \left| f_{7}(q^{2}) \right|^{2} m^{2}M_{\phi}^{2}\lambda + (2m^{2} + q^{2}) \left| (M_{B_{s}}^{2} - M_{\phi}^{2} - q^{2})f_{2}(q^{2}) + \lambda f_{3}(q^{2}) \right|^{2} + (q^{2} - 4m^{2}) \left| (M_{B_{s}}^{2} - M_{\phi}^{2} - q^{2})f_{5}(q^{2}) + \lambda f_{6}(q^{2}) \right|^{2} \right]$$
(69)

$$A_{\pm} = (q^2 - 4m^2) \left| f_5(q^2) \mp \sqrt{\lambda} f_4(q^2) \right|^2 + \left(q^2 + 2m^2 \right) \left| f_2(q^2) \pm \sqrt{\lambda} f_1(q^2) \right|^2$$
(70)

Finally the longitudinal and transverse helicity amplitude becomes

$$f_{L}(q^{2}) = \frac{d\Gamma_{L}(q^{2})/dq^{2}}{d\Gamma(q^{2})/dq^{2}}$$

$$f_{\pm}(q^{2}) = \frac{d\Gamma_{\pm}(q^{2})/dq^{2}}{d\Gamma(q^{2})/dq^{2}}$$

$$f_{T}(q^{2}) = f_{+}(q^{2}) + f_{-}(q^{2})$$
(71)

so that the sum of the longitudinal and transverse helicity amplitudes is equal to one i.e. $f_L(q^2) + f_T(q^2) = 1$ for each value of $q^2[24]$.

V. NUMERICAL ANALYSIS

In this section we will examine the above derived physical observables and analyze the effects of different new physics scenarios on them. Form factors which are the non perturbative quantities and for them we rely on the Light Cone Sum Rule (LCSR) approach for the numerical calculations. The numerical values of the LCSR form factors along with the different fitting parameters [53] are summarized in Table I. In addition to the parameters corresponding to different NP models there are some standard inputs which are collected in Table III.

TABLE III: Default values of input parameters used in the calculations.

$$\begin{split} m_{B_s} &= 5.366 \text{ GeV}, \ m_b = 4.28 \text{ GeV}, \ m_s = 0.13 \text{ GeV}, \\ m_\mu &= 0.105 \text{ GeV}, \ m_\tau = 1.77 \text{ GeV}, \ f_B = 0.25 \text{ GeV}, \\ |V_{tb}V_{ts}^*| &= 45 \times 10^{-3}, \ \alpha^{-1} = 137, \ G_F = 1.17 \times 10^{-5} \text{ GeV}^{-2}, \\ \tau_B &= 1.54 \times 10^{-12} \text{ sec}, \ m_\phi = 1.020 \text{ GeV}. \end{split}$$

The strength of the other NP parameters that corresponds to the UED and Z' model are varied such that they lie inside the bounds given by different flavor decays observed so for. It is emphasis here that in all the figures the band corresponds to the uncertainties in different input parameters where form factors are the main contributors (c.f. Table I) and we defined $q^2 = s$. The NP curves are plotted by varying the values of NP parameters in the range summarized in the Table IV.

Semileptonic B_s decay are ideal probes to study the physics in and beyond the Standard Model. In this context, there are large number of observables which are accessible in these decays. However, the branching ratio, in general for semi-leptonic decays like, is prune to many sources of uncertainties. The major source of uncertainty originate from the $B \rightarrow \phi$ transition form factors that can bring about 20 - 30% uncertainty to the differential branching ratio. This goes to show that differential branching ratio may not be a suitable observable to look for the NP effects unless these effects are very drastic. In the absence of the precise form factors, it is still possible to constraint new physics with the help of observables that exhibits reduced sensitivity to the form factors. In this regard the most important observables are the zero position of the forward-backward asymmetry, different lepton polarization asymmetries and the helicity fractions of the final state meson. This will become clear from Figs. 2-14, where we will see that the gray band corresponding to the uncertainties in different input parameters totally shrinks.

The SM predicts the zero crossing of $\mathcal{A}_{FB}(q^2)$ at a well determined position which is free from the hadronic uncertainties at the leading order (LO) in strong coupling α_s [12–14]. For this reason, the zero position of \mathcal{A}_{FB} , is an important observable in the search of new physics. In order to make this point clear, the zero position (q_0^2) is just the root of the Eq. (46), which can be written as

$$q_0^2 = -\frac{C_7^{eff}}{\Re \left(C_9^{eff} \left(q_0^2 \right) \right)} m_b \left[\frac{T_2 \left(q_0^2 \right)}{A_1 \left(q_0^2 \right)} \left(M_{B_s} - M_\phi \right) + \frac{T_1 \left(q_0^2 \right)}{V \left(q_0^2 \right)} \left(M_{B_s} + M_\phi \right) \right].$$
(72)

It is really spectacular that for the $B \to V l^+ l^-$ decays, we can find that with the use of effective theories like Soft Collinear Effective Theory (SCET) both ratios of the form factors appearing in Eq. (72) have no hadronic uncertainty,

i.e., all dependence on the intrinsically non-perturbative quantities cancels. Therefore, one can simply write

$$\frac{T_2(q^2)}{A_1(q^2)} = \frac{M_{B_s}}{M_{B_s} - M_{\phi}}$$
$$\frac{T_1(q^2)}{V(q^2)} = \frac{M_{B_s}}{M_{B_s} + M_{\phi}}$$

and using these relations, the short distance expression for the zero position \mathcal{A}_{FB} is given by [13]

$$q_0^2 = \frac{2m_b M_{B_s}}{\Re[C_9^{eff}(q_0^2)]} C_7^{eff}$$
(73)

Recently LHCb has published its results on $\mathcal{A}_{FB}(\bar{B} \to \bar{K}^* \mu^+ \mu^-)$ which shows, with small error bars, that the zero position of $\mathcal{A}_{FB}(\bar{B} \to \bar{K}^* \mu^+ \mu^-)$ is close to the SM's zero position. Like $\bar{B} \to \bar{K}^* \mu^+ \mu^-$ decay, the semileptonic decay $B_s \to \phi \mu^+ \mu^-$ also occurs through the quark level transition $b \to s \mu^+ \mu^-$. Therefore, the future measurements of the $\mathcal{A}_{FB}(B_s \to \phi \mu^+ \mu^-)$ will shed more light on the NP in the flavor sector.

The other "optimized" observables are the various polarization asymmetries attached to the final state leptons and meson where the uncertainties are also mild. Regarding this the longitudinal and normal lepton polarization asymmetries are the good tool to probe the NP. On the other hand, the transverse lepton polarization asymmetry (c.f. Eq. (53)) is proportional to the imaginary part of the auxiliary functions and hence will be negligible in the models where we have the real couplings. In addition to the single lepton polarization, we will also discuss the dependence of double lepton polarization asymmetries on q^2 and will also give the numerical values of their averages that can be obtained after integration on q^2 .

Another interesting observable in this list is the study of the spin effects of final state meson which for our case is the ϕ meson. A detailed discussion about the NP effects on the longitudinal and transverse helicity fractions has been done in the forthcoming numerical analysis which will provide help to dig out the potential of various NP scenarios.

Similarly, the polarized and unpolarized CP violating asymmetries are useful tool to find the distinguishing feature from the SM as well as will help us to segregate the two NP models. It is worth mentioning that the FCNC transitions are proportional to the CKM matrix elements, $V_{tb}V_{ts}^*$, $V_{cb}V_{cs}^*$ and $V_{ub}V_{us}^*$, where the later two are highly suppressed compared to the $V_{tb}V_{ts}^*$. This will eventually suppress the value of CP violation asymmetries in the SM and also in the UED model. Because of the extra phase in the Z' model we are expecting a prominent deviation. Therefore, the study of the CP violation asymmetries will provide a key evidence of the NP coming through the extra Z' boson. This will be discussed as a separate study which will be presented in [92].

The only free parameter in the UED model is the inverse of the compactification radius i.e. 1/R. Taking into account the leading order (LO) contributions due to the exchange of KK modes as well as already available next-to-next-to-leading order (NNLO) corrections to $B \to X_s \gamma$ the Haisch et al. [93] have obtained the lower bound on inverse of compactification radius to be 600 GeV. Using the electroweak precision measurements and also some cosmological constraints, the lower limit on the inverse of the the compactification radius is obtained to be in or above the 500 GeV range [94, 95]. It is well known that by increasing 1/R the values of different physical observables becomes closer to the SM values. Therefore, in our numerical analysis we take the value of 1/R to be 500 GeV just to see the maximum possible definition from the SM value.

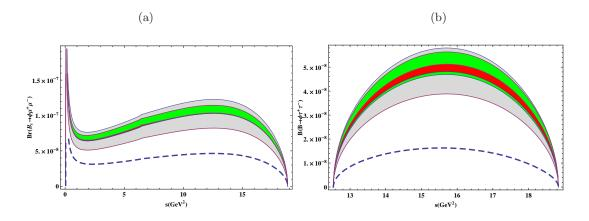
On the other hand the effects of the family non-universal Z' boson on $b \to s$ transition have attracted much more attention and been widely studied where it is argued that the behaviour of a family non-universal Z' boson is helpful to resolve many puzzles in B meson decays, such as πK puzzle and anomalous $\bar{B}_s - B_s$ mixing [98–102]. In literature the differential decay width and forward backward asymmetry of $B_s \to \phi \mu^+ \mu^-$ decay have been studied in the Z'model using three different scenarios which corresponds to different values of the the left and right handed couplings of Z' with leptons, i.e. S_{LL} and D_{LL} , as well as the right handed coupling with quarks, i.e., B_{sb} and these are collected in Table IV [102]. In the present study we will use these limits to see their impact on the branching ratio and to various asymmetries mentioned above.

TABLE IV: The numerical values of the Z^\prime parameter.

	$ B_{sb} \times 10^{-3}$	$\phi_{sb}[^o]$	$S_{LL} \times 10^{-2}$	$D_{LL} \times 10^{-2}$
\mathcal{S}_1	1.09 ± 0.22	-72 ± 7	-2.8 ± 3.9	-6.7 ± 2.6
\mathcal{S}_2	2.20 ± 0.15	-82 ± 4	-1.2 ± 1.4	-2.5 ± 0.9

The numerical results of the branching ratios, forward-backward asymmetry, different polarization asymmetries of the final state leptons, helicity fractions of the final state ϕ meson as a function of q^2 in $B_s \to \phi l^+ l^-$ decays are

FIG. 1: The differential width for the $B_s \to \phi l^+ l^ (l = \mu, \tau)$ decays as functions of $q^2 = s$. The gray, green and red bands corresponds to the Standard Model, Z' scenarios S_1 and S_2 respectively. The dashed blue line corresponds to the UED model.



presented in Figs. 1-14. Fig. 1(a,b) describes the differential branching ratio of $B_s \rightarrow \phi \mu^+ \mu^- (\tau^+ \tau^-)$ decay, where one can see that for the choice of the parameters made in accordance with the current data on various flavor physics decay modes lies close to the SM predictions. This can also be summarized in Table VII. Just to mention, when we have muon's as the final state leptons (c.f. Fig.1a) the bands for two Z' scenarios over lap with each other. We can also see that the value of the branching ratio lies well with in the range of the experimental limits with the choice of different values of NP parameters and one can notice that the NP contributions are over shadowed by the uncertainties involved in different input parameters. Therefore, to look for NP we have to calculate the observables where hadronic uncertainties almost have no effect and which are almost independent of the choice of form factors. Among them the most pertinent are the zero position of the forward-backward asymmetry, lepton polarization asymmetries, the helicity fractions of the final state meson and CP asymmetries, which being almost free from the hadronic uncertainties and serve as handy tools to extract NP signature.

TABLE V: Branching ratio of $B_s \rightarrow \phi l^+ l^-$ in SM and different NP scenarios. The central values of the form factors and other input parameters are used.

Model	$B_s \to \phi \mu^+ \mu^-$	$B_s \to \phi \tau^+ \tau^-$
SM	1.58×10^{-6}	2.37×10^{-7}
UED	0.91×10^{-6}	0.94×10^{-6}
Z'-	1.86×10^{-6}	3.07×10^{-7}

As we have already mentioned that at the leading order in the strong coupling constant α_s in the SM the destructive interference between the photon penguin (C_7^{eff}) and the Z penguin (C_9^{eff}) make the FBA equal to zero at a particular position which is independent of the form factors as depicted in Eq. (73). For the decay $B_s \rightarrow \phi \mu^+ \mu^-$, the value of the the zero crossing is approximately $(q^2 \simeq 1.6 \text{GeV}^2)$. The deviation of the zero crossing from the SM value gives us some clues for the NP. Fig. 2b shows the effect of various NP scenarios on the zero position of the forward-backward asymmetry for $B_s \rightarrow \phi \mu^+ \mu^-$ decay. Playing on the pitch of $B \rightarrow K^* l^+ l^-$ where the experimental results of LHCb lies close to the SM value, we can see that only the small deviation from the SM zero position of \mathcal{A}_{FB} comes in case of the Z' model. In case of the UED model the value of the Wilson coefficient C_7 is significantly reduced whereas C_9 almost remains unaltered for 1/R = 500GeV. By looking at the Eq. (73) we can see that the zero position is directly proportional to C_7 therefore, we expect large deviation in the UED model and this is obvious from Fig. 2b. We expect that in future when more data will come from the LHCb the measurement of the forward-backward asymmetry in $B_s \rightarrow \phi \mu^+ \mu^-$ will help us in observing new physics and will also give us an opportunity to distinguish between various NP scenarios.

It has been pointed out by Beneke et al. in ref. [14] that the Next-to-Leading Order (NLO) corrections to the lepton invariant mass spectrum in $B \to K^* l^+ l^-$ is small but there is a large correction to the predicted location of the zero position of the forward-backward asymmetry which is estimated to be 30%. Such calculation is still been waited for the $B_s \to \phi l^+ l^-$ decays before one can say anything about the NP by measuring forward-backward asymmetry in these decays.

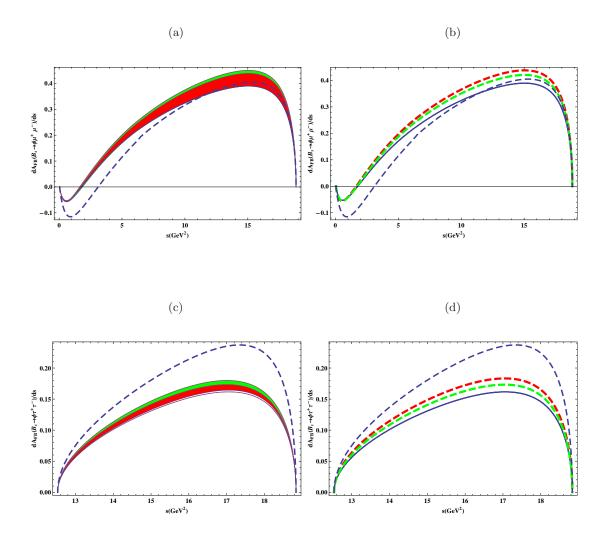


FIG. 2: The differential forward-backward asymmetry for the $B_s \rightarrow \phi l^+ l^ (l = \mu, \tau)$ decays as functions of q^2 . The gray, green and red bands corresponds to the Standard Model, Z' scenarios S_1 and S_2 respectively. The dashed blue line corresponds to the UED model. In Fig. 2(b,d) the solid, dashed-blue, dashed-green and dashed-red lines corresponds to SM, UED model, and Z' models scenario-I and II, respectively. Here the central values of the form factors and other input parameters are used.

Fig. 3(a,b,c,d) shows the dependence of longitudinal lepton polarization asymmetry for the $B_s \rightarrow \phi l^+ l^-$ decay on the square of momentum transfer for different NP models. In case of the UED model, the value of the longitudinal lepton polarizations lies close to the SM value where as significant deviation is obtained in case of the Z' model. This can also be seen quantitatively from Table VI, where 11% deviation is observed in case of the Z' model for the central values of its parameters.

Fig. 4(a,b,c,d) displays the behavior of normal lepton polarization asymmetry for the $B_s \rightarrow \phi l^+ l^-$ with square of momentum transfer in SM and in NP models. From Eq. (52) one can see that it is proportional to the mass of leptons. Therefore, when we have the muons as a final state leptons we can see that its SM value and the deviation from this value through NP are only significant at low q^2 region and these effects are almost vanishes when we increase the values of q^2 . is small. Similarly, we have drawn normal lepton polarization asymmetry when tau's are the final state leptons in Fig. 6(c,d). We can see that in SM the value of normal lepton polarization asymmetry is positive almost throughout the kinematical region. It can be easily seen that the value in the Z' model is also quite different from that of the SM value. The most interesting effects comes in the UED model where the value of this asymmetry is negative in almost all the available q^2 range. Hence it will be a clear signal of new physics and by measuring its sign we can distinguish between the under consideration NP models.

Just like the normal lepton polarization asymmetry the transverse lepton polarization asymmetry is also proportional

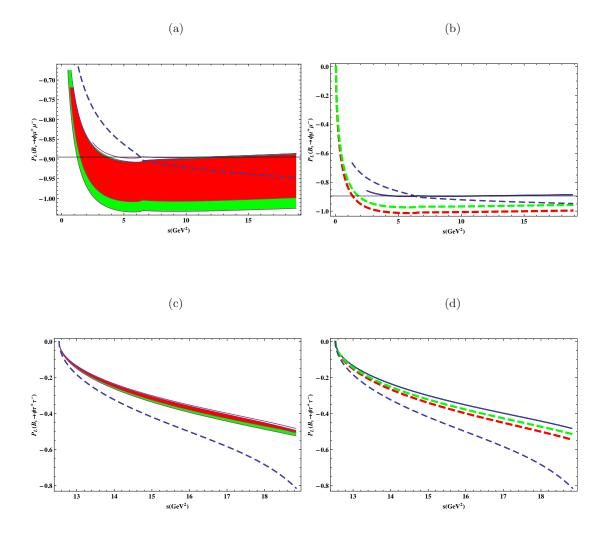


FIG. 3: The longitudinal lepton polarization asymmetry for the $B_s \to \phi l^+ l^ (l = \mu, \tau)$ decays as functions of q^2 . The legends are same as in Fig.2.

to the lepton mass. In addition to this it is also proportional to the imaginary part of the combination of different auxiliary functions and so of the Wilson coefficients. The Wilson coefficients remains real in the SM and UED model but not in the Z' model. However, in this model imaginary part is also too small. Hence the value of transverse lepton polarization asymmetry remains very small to be measured and Fig. 5(a,b,c,d) portrays this fact.

TABLE VI: Average values of various single lepton polarizations for the central values of the input parameters. The values in the bracket are for the $\tau^+\tau^-$ channel.

Model	$\langle P_L \rangle$	$\langle P_N \rangle$	$\langle P_T \rangle$
SM	-0.859(-0.322)	-0.0334(0.068)	0.0003(0.0028)
UED	-0.857(-0.462)	-0.0451(-0.197)	0.0007(0.0091)
$Z'(S_1)$	$-0.972^{+0.108}_{-0.024}(-0.365^{+0.031}_{+0.075})$	$-0.0445^{+0.007}_{-0.001}(0.023^{+0.019}_{+0.016})$	$-0.0005^{+0.005}_{-0.004}(0.0012^{+0.035}_{-0.023})$
$Z'(S_2)$	$-0.931^{0.066}_{-0.037}(-0.346^{+0.018}_{-0.001})$	$-0.040^{+0.001}_{-0.002}(0.046^{+0.012}_{+0.009})$	$-0.0006^{+0.004}_{-0.0036}(-0.0004^{+0.0023}_{-0.021})$

The dependence of various double lepton polarization asymmetries on q^2 for the aforementioned decay in SM and various NP scenarios is given in Fig. (6-12). In Fig. 6(a,b,c,d) we have plotted P_{LL} as a function of q^2 . It is clear from Eq. (58) that double longitudinal lepton polarization asymmetry is proportional to inverse of the mass of lepton,

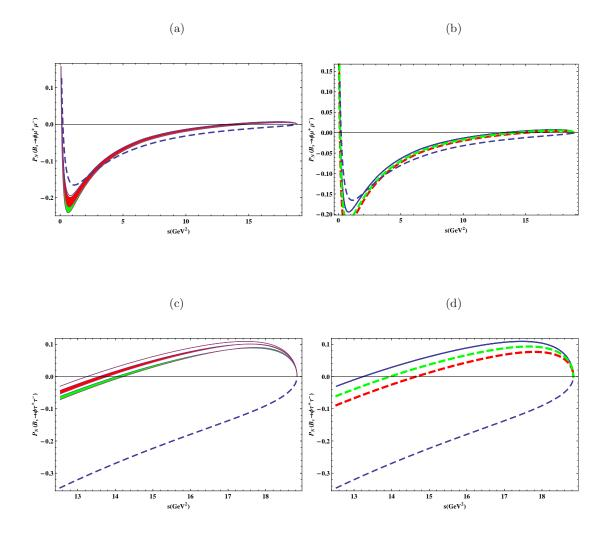


FIG. 4: The Normal lepton polarization asymmetry $B_s \rightarrow \phi l^+ l^ (l = \mu, \tau)$ decays as functions of q^2 . The legends are same as in Fig.2.

therefore it is expected to have a large value when final state leptons are the muons compared to the case when we have tauons and it is also clear from Fig. 6(a,b,c,d). We can also see that the dependency of P_{LL} on NP parameters is small for the μ -channel. However for the τ -channel the maximum shift comes in the Z' model where $\langle P_{LL} \rangle$ deviate almost an order of magnitude from the SM value (c.f. Table VII). Its measurement will help us in identifying the NP effects arising due to the extra gauge boson in the Z' model.

By looking at Eq. (7), we can see that P_{LN} is proportional to the imaginary part of the different auxiliary functions and so of the Wilson coefficients, therefore, its non zero value is expected only in the Z' model. However the imaginary part in this cases is small, therefore its values is expected to be small and Fig. 7(a,b) displays this fact which quantitatively can also be seen in Table VII.

Fig. 8(a,b,c,d) depicts the behavior of P_{LT} with q^2 where we can see that the new physics effects are quite promising both for the μ and τ -channels in almost whole range of available q^2 . Quantitatively we can see from Table VII that the value of average $\langle P_{LT} \rangle$ in UED model is closed to the SM value where as in the Z' model the average value of P_{LT} is significantly suppressed in magnitude from its SM value as well as it flips its sign for the τ channel.

In Fig. 9(a,b,c,d) we displayed the effects of various NP models on the P_{NN} . We can see that the value of P_{NN} shows strong dependence on the parameters of NP which is quite prominent in both μ and τ -channels. From Table VII, it is clear that in the Z' model the value of P_{NN} is significantly different not only from the SM value but also from the UED model. Therefore the experimental observation of this observable will help us to segregate the Z' model

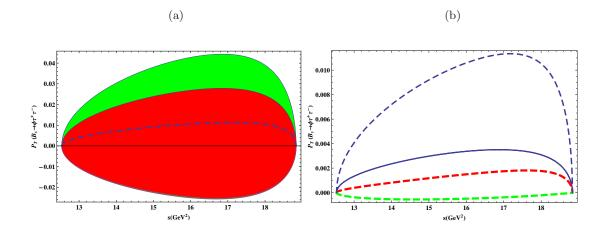


FIG. 5: The transverse lepton polarization asymmetry for the $B_s \to \phi l^+ l^ (l = \mu, \tau)$ decays as functions of q^2 . he legends are same as in Fig.2.

	$_{\rm SM}$	UED	$Z'(S_1$ -Scenario)	$Z'(S_2$ -Scenario)
$\langle P_{LL} \rangle$	-0.956(-0.046)	-0.939(-0.017)	$-0.961^{+0.003}_{-0.001} \left(-0.30^{+0.02}_{-0.025}\right)$	$-0.959^{+0.001}_{-0.006} \left(-0.313^{+0.011}_{-0.058}\right)$
$\langle P_{NN} \rangle$	0.014(0.153)	-0.066(0.192)	$-0.241^{+0.002}_{-0.014} \left(-0.166^{+0.021}_{-0.029}\right)$	$-0.265^{+0.005}_{-0.005} \left(-0.181^{+0.014}_{-0.023}\right)$
$\langle P_{TT} \rangle$	0.025(-0.207)	-0.037(-0.237)	$-0.218^{+0.005}_{-0.013} \left(0.102^{-0.021}_{+0.026}\right)$	$-0.238^{+0.005}_{-0.042} \left(0.114^{-0.013}_{+0.046}\right)$
$\langle P_{LN} \rangle$	0.0027(0.057)	0.0023(0.055)	$0.0028^{+0.021}_{-0.0138} \left(0.017^{+0.104}_{-0.067} \right)$	$0.0014^{+0.014}_{-0.002} \left(0.011^{+0.068}_{-0.060} \right)$
$\langle P_{LT} \rangle$	-0.069(-0.104)	-0.070(-0.104)	$-0.022^{-0.004}_{+0.003} \left(0.030^{-0.037}_{+0.015}\right)$	$-0.019^{-0.003}_{+0.002} \left(0.031^{-0.014}_{+0.014}\right)$
$\langle P_{TL} \rangle$	0.085(0.356)	0.084(0.356)	$0.050^{-0.001}_{-0.003} \left(0.180^{-0.001}_{-0.016} \right)$	$0.045^{+0.0001}_{-0.0001} \left(0.167^{+0.0001}_{-0.011} \right)$
$\langle P_{TN} \rangle$	0.0016(-0.0018)	-0.007(-0.0015)	$0.039^{+0.023}_{-0.011} \left(0.0058^{-0.0057}_{+0.004} \right)$	$0.037^{+0.007}_{-0.006} \left(0.0055^{-0.0054}_{+0.004}\right)$

TABLE VII: The values of double lepton polarizations for $\mu(\tau)$ in $B_s \to \phi \ell^+ \ell^-$ decays.

both from the SM as well as from UED model.

The situation for the P_{TL} is not so interesting for μ - channel because its average value is small in this case. However when we have τ 's as final state leptons, the effects of extra gauge boson in Z' model reduce the average value of P_{TL} by 50%. This can be seen quantitatively from Table VII and it is also depicted in Fig. 10(a,b,c,d).

In Eq. (11) we can see that the value of P_{TN} comes from the imaginary part of various Wilson Coefficients, therefore, as expected its value is too small to measure. This is obvious from Fig. 10(a,b,c,d) and also from Table VII.

The case in which both the leptons are transversely polarized that is P_{TT} becomes important for the τ channel. Here we can see that its behavior with q^2 is very different in the Z' model where it has positive values compared to its values in the SM and in UED model where the value of P_{TT} is negative. This fact is depicted in Fig. 12(a,b,c,d) and numerically given in Table VII.

The longitudinal (f_L) and the transverse (f_T) helicity fractions of final state ϕ meson are depicted in Figs. 13 and 14. In Figure 13 one can see that the values of longitudinal helicity fractions shifts significantly for some of the NP scenarios when we have taus' as the final state particles. The maximum deviation comes in the UED model and the reason is the significant modification of the Wilson coefficients C_7 and C_9 in this model compared to their SM values. Similar effects can also be seen in case of the transverse helicity fractions.

Just to summarize, in the present study we have observed the sizeable difference between the predictions of various physical observables in the SM and two different beyond the SM scenarios, namely, Z' and UED models. Keeping in view that in certain physical observables the NP effects are obscured by the uncertainties arising due to form factors but in different lepton polarization asymmetries their effects are still considerable. We hope that the experimental study of this channel will be a valuable source which provide an indirect way to dig out the new physics effects in an indirect way.

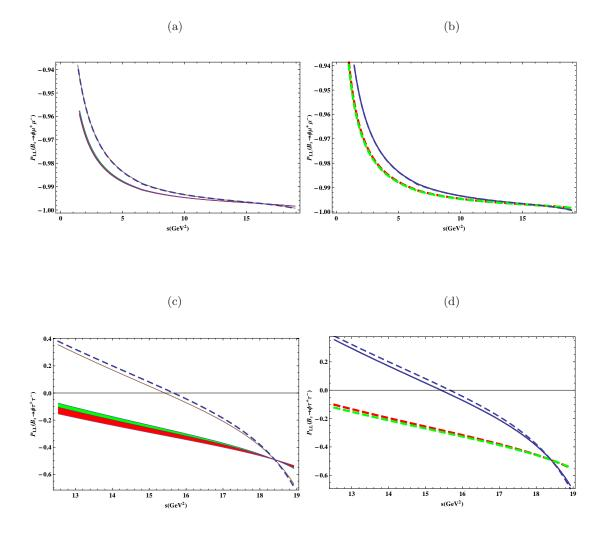


FIG. 6: P_{LL} for the $B_s \to \phi l^+ l^ (l = \mu, \tau)$ decays as functions of q^2 . The legends are same as in Fig.2.

Acknowledgments

The authors would like to thank Prof. Riazuddin and Prof. Fayyazuddin for their valuable guidance and helpful discussions. The author M. J. A would like to thank the support by Quaid-i-Azam University through the University Research Fund. MAP would like to acknowledge the grant (2012/13047-2) from FAPESP.

[6] E. Lunghi and A. Soni, Hints for the scale of new CP-violating physics from B-CP anomalies, JHEP 0908, 051 (2009)

S. L. Glashow, J. Iliopoulos, and L. Maiani, Weak Interactions with Lepton-Hadron Symmetry, Phys. Rev. D 2 (1970) 1285.

^[2] N. Cabibbo, Unitary Symmetry and Leptonic Decays, Phys. Rev. Lett. 10 (1963) 531.

^[3] M. Kobayashi and K. Maskawa, Symmetry breaking of chiral $U(3) \otimes U(3)$ and $X \to \eta \pi \pi decay$ amplitude, Prog. Theor. Phys. 49 (1973) 652.

^[4] H. Y. Cheng, C. K. Chua and A. Soni, CP-violating asymmetries in B0 decays to K+ K- K0(S(L)) and K0(S) K0(S) K0(S(L)), Phys. Rev. D 72, 094003 (2005) [arXiv:hep-ph/0506268].

^[5] G. Buchalla, G. Hiller, Y. Nir and G. Raz, The Pattern of CP asymmetries in $b \rightarrow s$ transitions, JHEP **0509**, 074 (2005) [arXiv:hep-ph/0503151].

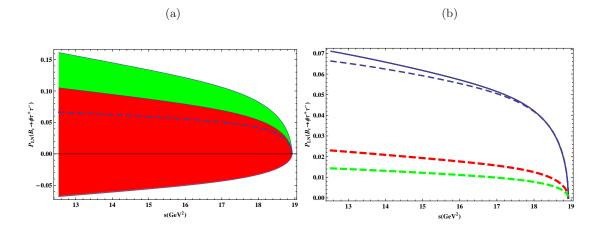


FIG. 7: P_{LN} for the $B_s \to \phi l^+ l^ (l = \mu, \tau)$ decays as functions of q^2 . The legends are same as in Fig.2.

[arXiv:0903.5059 [hep-ph]].

- [7] E. Barberio et al. [Heavy Flavor Averaging Group], Averages of b-hadron and c-hadron Properties at the End of 2007, arXiv:0808.1297 [hep-ex].
- [8] M. Bona *et al.* [UTfit Collaboration], First Evidence of New Physics in $b \leftrightarrow s$ Transitions, PMC Phys. A **3**, 6 (2009) [arXiv:0803.0659 [hep-ph]].
- [9] S. Baek, C. W. Chiang and D. London, Phys. Lett. B 675 (2009) 59.
- [10] T. Feldmann and J. Matias, J. High Energy Phys. 0301 (2003) 074 [hep-ph/0212158]; B. Aubert et al. [BABAR Collaboration], Phys. Rev. Lett. 102 (2009) 091803 [arXiv:0807.4119 [hep-ex]].
- [11] Ken Kiers, Tal Knighton, David London, Matthew Russell, Alejandro Szynkman and Kari Webster, Using $t \to b\bar{b}c$ to Search for New Physics, arXiv: 1107.0754 [hep-ph].
- [12] G. Burdman, Short distance coefficients and the vanishing of the lepton asymmetry in $B \rightarrow V \ell^+$ lepton, Phys. Rev. D 57, 4254 (1998) [arXiv:hep-ph/9710550].
- [13] A. Ali, P. Ball, L. T. Handoko and G. Hiller, A Comparative study of the decays $B \to (K, K^*)\ell^+\ell^-$ in standard model and supersymmetric theories, Phys. Rev. D **61**, 074024 (2000) [arXiv:hep-ph/9910221].
- [14] M. Beneke, T. Feldmann and D. Seidel, Systematic approach to exclusive $B \rightarrow V\ell + \ell -$, $V\gamma$ decays, Nucl. Phys. B **612**, 25 (2001) [arXiv:hep-ph/0106067].
- [15] R. Aaij, LHCb Collaboration, Differential branching fraction and angular analysis of the decay $B^0 \to \bar{K}^{0*} \mu^+ \mu^-$, Phys. Rev. Lett. **108** (2012) 181806.
- [16] A.Ishikawa et al., Measurement of forward-backward asymmetry and Wilson coefficients in $B \to K^* l^+ l^-$, Phys. Rev. Lett. 96 (2006) 251801 [hep-ex/0603018].
- [17] J. T. Wei et al. [BELLE Collaboration], Measurement of the differential branching fraction and forward-backward asymmetry for $B \to K^{(*)}\ell^+\ell^-$ Phys. Rev. Lett. **103** (2009) 171801 [arXiv:0904.0770 [hep-ex]].
- [18] B. Aubert et al. [BABAR Collaboration], Measurements of branching fractions, rate asymmetries, and angular distributions in the rare decays $B \to K \ell^+ \ell^-$ and $B \to K^* \ell^+ \ell^-$, Phys. Rev. D 73, 092001 (2006) [arXiv:hep-ex/0604007].
- [19] A. S. Cornell, N. Gaur and S. K. Singh, FB asymmetries in the $B \to K^* \ell + \ell decay$: A Model independent approach, arXiv:hep-ph/0505136.
- [20] A. Ali, T. Mannel and T. Morozumi, Forward backward asymmetry of dilepton angular distribution in the decay $b \rightarrow s\ell + \ell -$, Phys. Lett. B 273, 505 (1991).
- [21] A. J. Buras and M. Munz, Effective Hamiltonian for $B \to X_s e^+ e^-$ beyond leading logarithms in the NDR and HV schemes, Phys. Rev. D 52, 186 (1995) [arXiv:hep-ph/9501281].
- [22] M. Misiak, The $b \rightarrow se^+e^-$ and $b \rightarrow s\gamma$ decays with next-to-leading logarithmic QCD corrections, Nucl. Phys. B **393**, 23 (1993) [Erratum-ibid. B **439**, 461 (1995)].
- [23] F. Kruger and E. Lunghi, Looking for novel CP violating effects in $\overline{B} \to K^* \ell^+$ lepton, Phys. Rev. D 63, 014013 (2001) [arXiv:hep-ph/0008210].
- [24] A. Ali, E. Lunghi, C. Greub and G. Hiller, Improved model independent analysis of semileptonic and radiative rare B decays, Phys. Rev. D 66, 034002 (2002) [arXiv:hep-ph/0112300].
- [25] A. Ghinculov, T. Hurth, G. Isidori and Y. P. Yao, New NNLL results on the decay $B \to X_s l^+ l^-$, Eur. Phys. J. C 33, S288 (2004) [arXiv:hep-ph/0310187].
- [26] C. Bobeth, T. Ewerth, F. Kruger and J. Urban, Analysis of neutral Higgs boson contributions to the decays $\bar{B}(s) \rightarrow \ell^+ \ell^-$

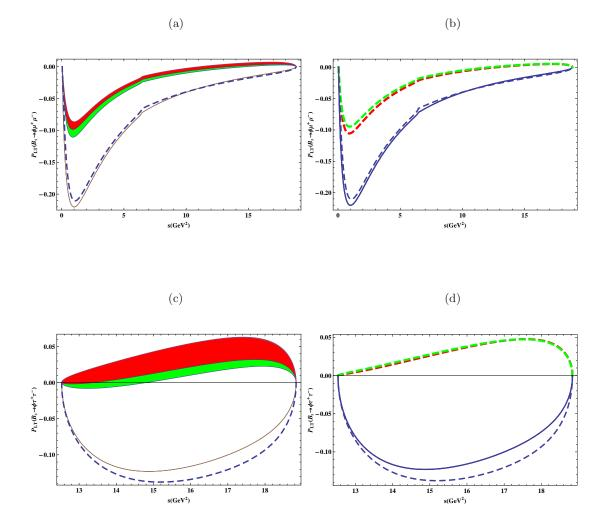


FIG. 8: P_{LT} for the $B_s \to \phi l^+ l^ (l = \mu, \tau)$ decays as functions of q^2 . The legends are same as in Fig.2.

and $\bar{B} \to K \ell^+ \ell^-$, Phys. Rev. D 64, 074014 (2001) [arXiv:hep-ph/0104284].

- [27] P. H. Chankowski and L. Slawianowska, Effects of the scalar FCNC in $b \rightarrow sl^+l^-$ transitions and supersymmetry, Eur. Phys. J. C 33, 123 (2004) [arXiv:hep-ph/0308032].
- [28] G. Hiller and F. Kruger, More model independent analysis of $b \rightarrow s$ processes, Phys. Rev. D 69, 074020 (2004) [arXiv:hep-ph/0310219].
- [29] A. K. Alok and S. U. Sankar, New physics upper bound on the branching ratio of $B_s \to \ell^+ \ell^-$, Phys. Lett. B **620**, 61 (2005) [arXiv:hep-ph/0502120].
- [30] Å. K. Ålok, A. Dighe and S. U. Sankar, Tension between scalar/pseudoscalar new physics contribution to $B_{(s)} \rightarrow \mu^+ \mu^$ and $B \rightarrow K \mu^+ \mu^-$ Mod. Phys. Lett. A 25, 1099 (2010) [arXiv:0803.3511 [hep-ph]].
- [31] A. K. Alok, A. Dighe and S. U. Sankar, Probing extended Higgs sector through rare $b \rightarrow s\mu^+\mu^-$ transitions, Phys. Rev. D 78, 034020 (2008) [arXiv:0805.0354 [hep-ph]].
- [32] A. Hovhannisyan, W. S. Hou and N. Mahajan, $B \to K^* \ell^+ \ell^-$ Forward-backward Asymmetry and New Physics, Phys. Rev. D 77, 014016 (2008) [arXiv:hep-ph/0701046].
- [33] F. Kruger and J. Matias, Probing new physics via the transverse amplitudes of $B_0 \to K_0^* (\to K^- \pi^+) \ell^+ \ell^-$ at large recoil, Phys. Rev. D **71**, 094009 (2005) [arXiv:hep-ph/0502060].
- [34] E. Lunghi and J. Matias, Huge right-handed current effects in $B \to K^*(\to K\pi)\ell^+\ell^-$ in supersymmetry, JHEP 0704, 058 (2007) [arXiv:hep-ph/0612166].
- [35] U. Egede, T. Hurth, J. Matias, M. Ramon and W. Reece, New observables in the decay mode $\bar{B}_d \to \bar{K}_0^* \ell^+ \ell^-$, JHEP **0811**, 032 (2008) [arXiv:0807.2589 [hep-ph]].
- [36] T. M. Aliev, V. Bashiry and M. Savci, Double lepton polarization asymmetries in the $B \to K \ell^+ \ell^-$ decay beyond the

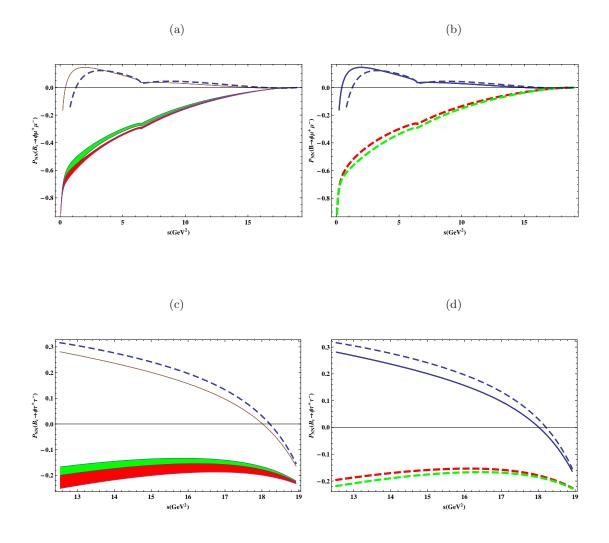


FIG. 9: P_{NN} for the $B_s \to \phi l^+ l^ (l = \mu, \tau)$ decays as functions of q^2 . The legends are same as in Fig.2.

standard model, Eur. Phys. J. C 35, 197 (2004) [arXiv:hep-ph/0311294].

- [37] T. M. Aliev, V. Bashiry and M. Savci, Polarized lepton pair forward backward asymmetries in $B \to K^* \ell^+ \ell^-$ decay beyond the standard model, JHEP 0405, 037 (2004) [arXiv:hep-ph/0403282].
- [38] T. M. Aliev, M. K. Cakmak, A. Ozpineci and M. Savci, New physics effects to the lepton polarizations in the B → Kℓ⁺ℓ⁻ decay, Phys. Rev. D 64, 055007 (2001) [arXiv:hep-ph/0103039].
- [39] W. Bensalem, D. London, N. Sinha and R. Sinha, Lepton polarization and forward backward asymmetries in $b \to s\tau^+\tau^-$, Phys. Rev. D 67, 034007 (2003) [arXiv:hep-ph/0209228].
- [40] A. K. Kumar, A. Dighe, D. Ghosh, D. London, J. Matias, M. Nagashima and A. Sznkman, New Physics Contributions to the Forward-Backward Asymmetry in $B \to K^* \mu^+ \mu^-$ JHEP **02** (2010) 053.
- [41] CDF Collaboration, Measurement of forward-backward asymmetry in $B \to K^* \mu^+ \mu^-$ and first observation of $B_s^0 \to \phi \mu^+ \mu^-$, Phys. Rev. Lett. 106
- [42] R. Fleischer and R. Knegjens, Effective Lifetimes of B_s Decay and their Constraints on the $B_s^0 \bar{B}_s^0$ Mixing Parameters:arXiv:1109.5115 [hep-ph].
- [43] F. Azfar et al. [CDF Collaboration], Public Note 10206 (2010).
- [44] V. M. Abazov et al. [D0 Collaboration], arXiv: 1109.3166 [hep-ex].
- [45] R. Van Kooten, Talk at Lepton-Photon 2011, Mumbai, India, 22-27 August 2011 [http://www.tifr.res.in/lp11].
- [46] V. M. Abazov et al. [D0 Collaboration], arXiv: 1106.6308 [hep-ex]
- [47] G. Raven, Talk at Lepton-Photon 2011, Mumbai, India, 22-27 August 2011 [http://www.tifr.res.in/lp11].
- [48] U. O. Yilmaz, Analysis of $B_s \to \phi \ell^+ \ell^-$ decay with new physics effects, Eur. Phys. J. C 58, 555 (2008) [arXiv:0806.0269 [hep-ph]].

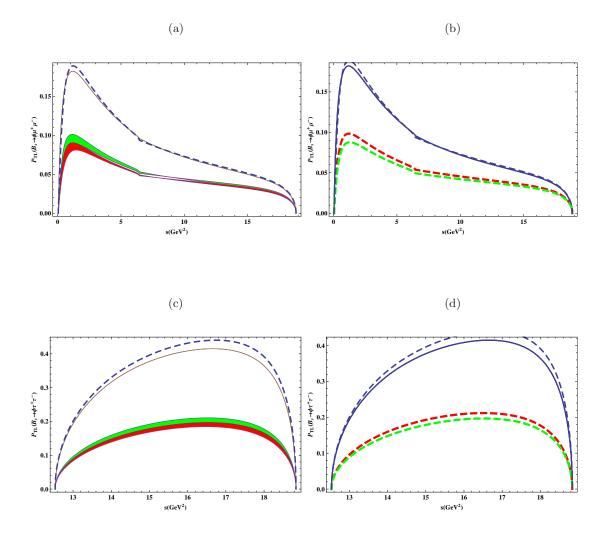


FIG. 10: P_{TL} for the $B_s \to \phi l^+ l^ (l = \mu, \tau)$ decays as functions of q^2 . The legends are same as in Fig.2.

- [49] G. Erkol and G. Turan, The Exclusive $B \to \phi \ell^+ \ell^-$ decay in the two Higgs doublet models, Eur. Phys. J. C 25, 575 (2002) [arXiv:hep-ph/0203038].
- [50] Q. Chang and Y. H. Gao, Probe a family non-universal Z' boson effects in $\bar{B}_s \to \phi \mu^+ \mu^-$ decay, Nucl. Phys. B 845, 179 (2011) [arXiv:1101.1272 [hep-ph]].
- [51] R. Mohanta and A. K. Giri, Study of FCNC mediated rare B_s decays in a single universal extra dimension scenario, Phys. Rev. D 75, 035008 (2007) [arXiv:hep-ph/0611068].
- [52] Ying Li and Juan Hua, arXiv: 1105.3031 [hep-ph].
- [53] P. Ball and V. M. Braun, Exclusive semileptonic and rare B meson decays in QCD, Phys. Rev. D 58, 094016 (1998) [arXiv:hep-ph/9805422].
- [54] P. Ball and R. Zwicky, $B_{d,s} \rightarrow \rho, \omega, K^*, \phi$ decay form-factors from light-cone sum rules revisited, Phys. Rev. D 71, 014029 (2005) [arXiv:hep-ph/0412079].
- [55] Y. L. Wu, M. Zhong and Y. B. Zuo, $B_s, D_s \to \pi, K, \eta, \rho, K^*, \omega, \phi$ Transition Form Factors and Decay Rates with Extraction of the CKM parameters -V(ub), -V(cs), -V(cd), Int. J. Mod. Phys. A **21**, 6125 (2006) [arXiv:hep-ph/0604007].
- [56] W. Wang, R. H. Li and C. D. Lu, Radiative charmless $B_s \to V\gamma$ and $B_s \to A\gamma$ decays in pQCD approach, arXiv:0711.0432 [hep-ph].
- [57] D. Melikhov and B. Stech, Weak form-factors for heavy meson decays: An Update, Phys. Rev. D 62, 014006 (2000) [arXiv:hep-ph/0001113].
- [58] A. Deandrea and A. D. Polosa, The Exclusive $B_s \to \phi \mu^+ \mu^-$ process in a constituent quark model, Phys. Rev. D 64, 074012 (2001) [arXiv:hep-ph/0105058].
- [59] C. Q. Geng and C. C. Liu, Study of $B_s \rightarrow (\eta, \eta', \phi) \ell \bar{\ell}$ decays," J. Phys. G 29, 1103 (2003) [arXiv:hep-ph/0303246].

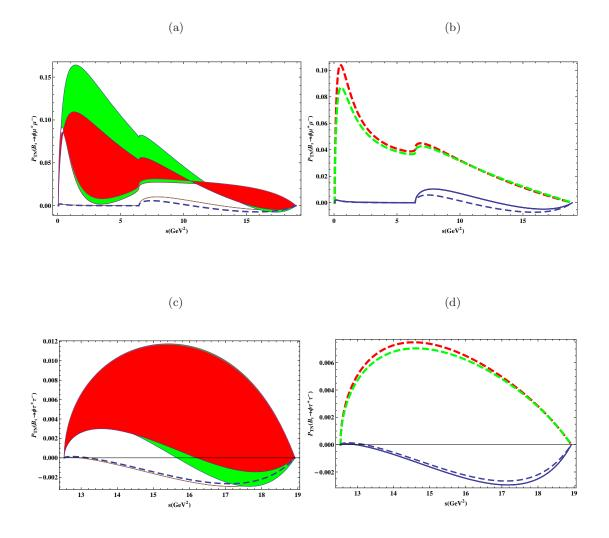


FIG. 11: P_{TN} for the $B_s \to \phi l^+ l^ (l = \mu, \tau)$ decays as functions of q^2 . The legends are same as in Fig.2.

- [60] C. M. Bouchard *et al Form factors for B and B_s semileptonic decays with NRQCD/HISQ quarks*, arXiv:1210.6992 [hep-lat].
- [61] G. Buchalla, A. J. Buras and M. E. Lautenbacher, Weak decays beyond leading logarithms, Rev. Mod. Phys. 68, 1125 (1996) [arXiv:hep-ph/9512380].
- [62] A. J. Buras and M. Munz, Effective Hamiltonian for $B \to X_s e^+e^-$ beyond leading logarithms in the NDR and HV schemes, Phys. Rev. D 52, 186 (1995) [arXiv:hep-ph/9501281].
- [63] C. S. Lim, T. Morozumi and A. I. Sanda, A Prediction for d gamma (b ¿ s Lepton anti-Lepton) / d q**2 Including the Long Distance Effects, Phys. Lett. B 218, 343 (1989).
- [64] A. Ali, T. Mannel and T. Morozumi, Forward backward asymmetry of dilepton angular distribution in the decay $b \rightarrow sl^+l^-$ Phys. Lett. B **273**, 505 (1991).
- [65] F. Kruger and L. M. Sehgal, Lepton polarization in the decays $B \to X_s \mu^+ \mu^-$ and $B \to X_s \tau^+ \tau^-$, Phys. Lett. B **380**, 199 (1996) [arXiv:hep-ph/9603237].
- [66] B. Grinstein, M. J. Savage and M. B. Wise, $B \to X_s e^+ e^-$ in the Six Quark Model, Nucl. Phys. B **319**, 271 (1989).
- [67] G. Cella, G. Ricciardi and A. Vicere, QCD corrections to the $\bar{B} \to X_s e^+ e^-$ decay, Phys. Lett. B 258, 212 (1991).
- [68] C. Bobeth, M. Misiak and J. Urban, Photonic penguins at two loops and m(t) dependence of BR[B X(s) lepton+ lepton-], Nucl. Phys. B 574, 291 (2000) [arXiv:hep-ph/9910220].
- [69] H. H. Asatrian, H. M. Asatrian, C. Greub and M. Walker, Two loop virtual corrections to B X(s) lepton+ lepton- in the standard model, Phys. Lett. B 507, 162 (2001) [arXiv:hep-ph/0103087].
- [70] M. Misiak, The $b \rightarrow se^+e^-$ and $b \rightarrow s\gamma$ decays with next-to-leading logarithmic QCD corrections, Nucl. Phys. B **393**, 23 (1993) [Erratum-ibid. B **439**, 461 (1995)].

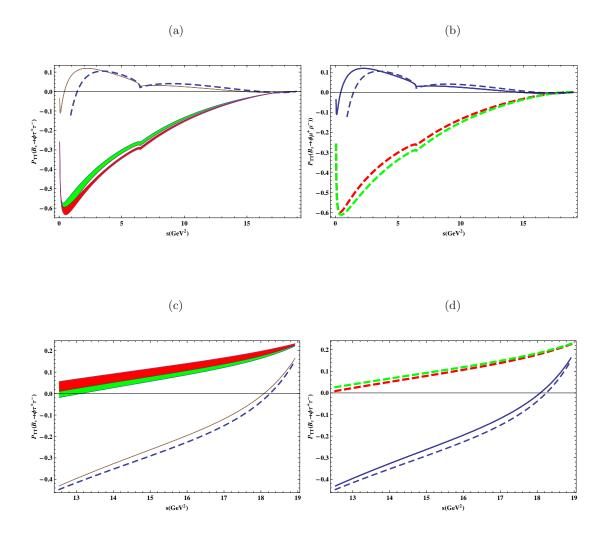


FIG. 12: P_{TT} for the $B_s \to \phi l^+ l^ (l = \mu, \tau)$ decays as functions of q^2 . The legends are same as in Fig.2.

- [71] D. Melikhov, N. Nikitin and S. Simula, Lepton asymmetries in exclusive $b \rightarrow sl^+l^-$ decays as a test of the standard model, Phys. Lett. B 430, 332 (1998) [arXiv:hep-ph/9803343].
- [72] J. M. Soares, CP violation in radiative b decays, Nucl. Phys. B 367, 575 (1991).
- [73] G. M. Asatrian and A. Ioannisian, CP violation in the decay $b \rightarrow s\gamma$ in the left-right symmetric model, Phys. Rev. D 54, 5642 (1996) [arXiv:hep-ph/9603318].
- [74] J. M. Soares, The contribution of the J / Psi resonance to the radiative B decays, Phys. Rev. D 53, 241 (1996) [arXiv:hep-ph/9503285].
- [75] C. H. Chen and C. Q. Geng, Baryonic rare decays of $\Lambda_b \to \Lambda l^+ l^-$, Phys. Rev. D 64, 074001 (2001) [arXiv:hep-ph/0106193].
- [76] T. Huber, T. Hurth and E. Lunghi, The Role of Collinear Photons in the Rare Decay $\bar{B} \to X_s \ell^+ \ell^-$, arXiv:0807.1940 [hep-ph].
- [77] D. Melikhov, N. Nikitin and S. Simula, Lepton asymmetries in exclusive $b \rightarrow sl^+l^-$ decays as a test of the standard model, Phys. Lett. B 430, 332 (1998) [arXiv:hep-ph/9803343].
- [78] J. M. Soares, CP violation in radiative b decays, Nucl. Phys. B 367, 575 (1991).
- [79] G. M. Asatrian and A. Ioannisian, CP violation in the decay $b \to s\gamma$ in the left-right symmetric model," Phys. Rev. D 54, 5642 (1996) [arXiv:hep-ph/9603318].
- [80] T. Appelquist, H. C. Cheng and B. A. Dobrescu, Bounds on universal extra dimensions, Phys. Rev. D64 (2001) 035002.
- [81] A. J. Buras, M. Spranger and A.Weiler, The Impact of Universal Extra Dimensions on the Unitarity Triangle and Rare K and B Decays, Nucl. Phys. B660 (2003) 225
- [82] A. J. Buras, A. Poschenrieder, M. Spranger and A.Weiler, The Impact of Universal Extra Dimensions on $B \to Xs\gamma$, $B \to Xsg$, $B \to Xs\mu^+\mu^-$, $K_L \to \pi^0 e^+ e^-$, and ε/ε' , Nucl. Phys. B678 (2004) 455.

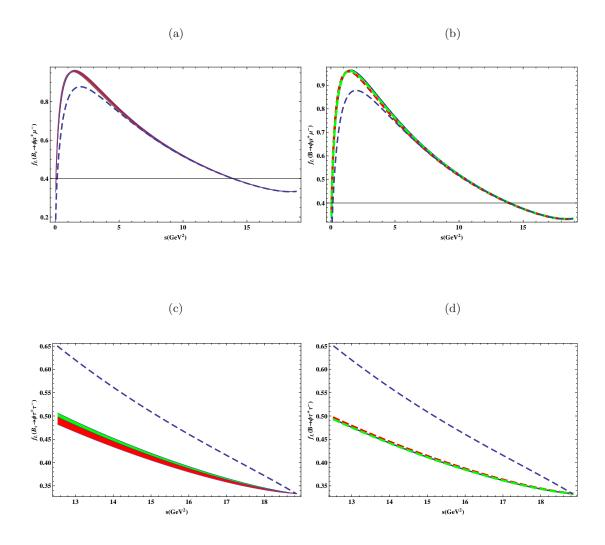


FIG. 13: The longitudinal helicity fractions for the $B_s \to \phi l^+ l^ (l = \mu, \tau)$ decays as functions of q^2 . The legends are same as in Fig.2.

- [83] K. Agashe, N. G. Deshpande and G. H. Wu, Universal Extra Dimensions and $b \rightarrow s\gamma$, Phys. Lett. B514 (2001) 309.
- [84] P. Langacker and M. Plumacher, "Flavor changing effects in theories with a heavy Z' boson with Phys. Rev. D 62, 013006 (2000) [arXiv:hep-ph/0001204].
- [85] V. Barger, L. Everett, J. Jiang, P. Langacker, T. Liu and C. Wagner, "Family Non-universal U(1)-prime Gauge Symmetries and b- > s Phys. Rev. D 80, 055008 (2009) [arXiv:0902.4507 [hep-ph]].
- [86] M.Jamil Aslam, Cai-Dian Lu and Yu-Ming Wang, $B \to K_0^* \ell^+ \ell^-$ decays in supersymmetric theories, Phys. Rev. D 79, 074007 (2009) [arXiv:0902.0432].
- [87] M.Jamil Aslam, Yu-Ming Wang and Cai-Dian Lu, Exclusive semileptonic decays of $\Lambda_b \to \Lambda \ell^+ \ell^-$ in supersymmetric theories, Phys. Rev. D 78, 114032 (2008) [arXiv:0808.2113].
- [88] T. M. Aliev and M. Savci, $\Lambda_b \to \Lambda \ell^+ \ell^-$ decay in universal extra dimensions, Eur. Phys. J. C 50,91 (2007) [arXiv: hep-ph/0606225].
- [89] P. Colangelo et al., Phys. Rev. D 74, (2006) 115006 [hep-ph/0610044]; A. Siddique et al., arXiv:0803.0192.
- [90] M. A. Paracha et al., arXiv:1101.2323 (2011).
- [91] V. Bashiry and K. Azizi, Systematic analysis of the $B_s \to f_0 \ell^+ \ell^-$ in the universal extra dimension, arXiv: 1112.5243 [hep-ph].
- [92] Ishtiaq Ahmed and M. Jamil Aslam, in prepration.
- [93] U. Haisch, A. Weiler, Bound on minimal universal extra dimensions from $\bar{B} \to X_s \gamma$, Phys. Rev. D 76, 034014 (2007).
- [94] I. Gogoladze and C. Macesanu, Precision electroweak constraints on Universal Extra Dimensions revisited Phys. Rev. D 74, 093012 (2006).

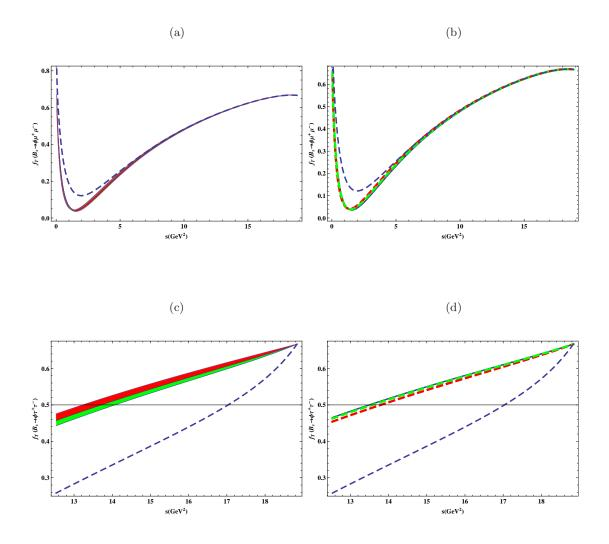


FIG. 14: The transverse helicity fractions for the $B_s \to \phi l^+ l^ (l = \mu, \tau)$ decays as functions of q^2 . The legends are same as in Fig.2.

- [95] J. A. R. Cembranos, J. L. Feng and L. E. Strigari, Exotic Collider Signals from the Complete Phase Diagram of Minimal Universal Extra Dimensions Phys. Rev. D 75, 036004 (2007).
- [96] T. Aaltonen et al. [CDF Collaboration], arXiv: 1103.2482 [hep-ex].
- [97] T. Aaltonen et al. [CDF Collaboration], Phys. Rev. Lett. 100, 161803 (2008); P. Q. Hung and M. Sher, Phys. Rev. D 77, 037302 (2008).
- [98] V. Barger, C. W. Chiang, P. Langacker and H. S. Lee, Solution to the $B \to \pi K$ Puzzle in a Flavor-Changing Z' Model, Phys. Lett. B 598 (2004) 218 [hep-ph/0406126].
- [99] Q. Chang, X. Q. Li and Y. D. Yang, Constraints on the nonuniversal Z' couplings from $B \to \pi K$, πK^* and ρK Decays, JHEP 0905 (2009) 056, arXiv:0903.0275 [hep-ph].
- [100] V. Barger, L. Everett, J. Jiang, P. Langacker, T. Liu and C. Wagner, Family Non-universal U' (1) Gauge Symmetries and $b \rightarrow s$ Transitions, Phys. Rev. D 80 (2009) 055008 arXiv:0902.4507 [hep-ph].
- [101] V. Barger, L. Everett, J. Jiang, P. Langacker, T. Liu and C. Wagner, $b \rightarrow s$ Transitions in Family-dependent U'(1) Models, JHEP 0912 (2009) 048, arXiv:0906.3745 [hep-ph].
- [102] Q. Chang, X. Q. Li and Y. D. Yang, Family Non-universal Z' effects on $\bar{B}_q B_q$ mixing, $B \to X_s \mu^+ \mu^-$ and $B_s \to \mu^+ \mu^-$ Decays, JHEP 1002 (2010) 082, arXiv:0907.4408 [hep-ph].